Distributed Dynamic Hydrological Modelling of Soil Erosion and Deposition

Implementing a function for soil erosion and deposition in a dynamic triangular flow algorithm (TFM-DYN)

Elias Haglund

Degree project/Independent project • 30 credits
Swedish University of Agricultural Sciences (SLU)
Faculty of Landscape Architecture, Horticulture and Crop Production Sciences
Department of Landscape Architecture, Planning and Management
Landscape Architecture Programme
Alnarp, 2024

Distributed Dynamic Hydrological Modelling of Soil Erosion and Deposition. Implementing a function for soil erosion and deposition in a dynamic triangular flow algorithm (TFM-DYN)

Distribuerad dynamisk hydrologisk modellering av markerosion och deposition. Implementering av en jorderosionsfunktion i en dynamisk triangular flödesalgoritm (TFM-DYN)

Elias Haglund

Supervisor:	**Abdulghani Hasan, Swedish University of Agricultural Sciences (SLU), Department of Landscape Architecture, Planning and Management**
Examiners:	Ishi Buffam & Christine Haaland, Dept. of Landscape Architecture, Planning and Management

Credits:	30 credits
Level:	A2E
Course title:	Independent Project in Landscape Architecture
Course code:	EX0846
Programme/education:	Landscape Architecture Programme
Course coordinating dept:	Dept. of Landscape Architecture, Planning and Management
Place of publication:	Alnarp
Year of publication:	2024
Copyright:	All featured images are used with permission from the copyright owner.

Keywords:	soil erosion model, rainfall-runoff modelling, flood modelling, soil deposition, soil erosion, environmental modelling, dynamic triangular flow algorithm, TFM-DYN, LISEM

Swedish University of Agricultural Sciences

Faculty of Landscape Architecture, Horticulture and Crop Production Sciences

Department of Landscape Architecture, Planning and Management

Abstract

Soil erosion and deposition are natural planetary phenomena. However, human activities such as conventional till agriculture and deforestation have increased the rate of erosion and subsequent soil degradation, consequently increasing the risks of for example global food insecurity. Also, eroded soil may be transported by waterways and deposit as sediment at locations where it can cause ecological or societal disturbances. As such, preventing erosion has become a prioritised policy globally in many sectors, and a strategic topic within the field of landscape architecture, planning and management.

Environmental models that estimate soil erosion and deposition by water are therefore of great importance. In landscape architecture, they can be used for spatial risk assessment to indicate erosion hotspots within a geographical area, and to recommend subsequent preventionary measures. Since the 20th century many attempts have been made to develop lumped or distributed models for such assessments, for example the LImberg Soil Erosion Model (LISEM). This study presents a prototype of, to my knowledge, the first soil erosion and deposition functionality added into a dynamic triangular flow algorithm (TFM-DYN). It uses a set of equations from LISEM implemented into TFM-DYN to estimate potential soil erosion, and sediment transport and deposition within a specific geographical area and time and uses data input regarding characteristics of the land and attributes of one or several rain events.

The results show that the added functionality generally meets the expected logic of erosion and deposition: soil is eroded based on the water's transport capacity and, as sediment, transported and deposited according to the flow distribution of the dynamic triangular flow algorithm. However, the model needs additional calibration for practical use, and more experimentation to adjust deposition rate estimation, and so leaves room for improvement.

Keywords: soil erosion model, rainfall-runoff modelling, flood modelling, soil deposition, soil erosion, environmental modelling, dynamic triangular flow algorithm, TFM-DYN, LISEM

Table of contents

List of tables

List of figures

Abbreviations

USLE	Universal Soil Loss Equation
LISEM	LImburg Soil Erosion Model
SFD	Single Flow Direction
MFD	Multiple Flow Direction
TIN	Triangular Irregular Network
TFM	Triangular Flow Model
TFM-DYN	Dynamic Triangular Flow Model
SOM	Soil Organic Matter
DEM	Digital Elevation Model
GIS	Geographical Information System
NED	Net Erosion and Deposition

1. Introduction

This introduction includes a background of soil erosion, its processes, consequences, and some currently existing soil erosion models and distributed hydrological models. The purpose, aim, goals, research questions and limitations are also presented.

1.1 Background

Soil erosion is the planetary process of separation and transport of soil particles by erosive agents like rainfall, surface runoff, wind, or gravity (Chapin et al. 2011). Naturally, the rate of erosion varies globally but tends to be balanced by other long-term natural processes of soil production (Montgomery 2007). While natural soil erosion can have negative consequences, deforestation, overgrazing, and agriculture have led to accelerated soil erosion (Borrelli 2017); for conventional tillage agriculture, the rate of soil erosion occurs 10 to 1000 times faster than naturally (Montgomery 2007; Caon & Vargas 2017). Over time, this can lead to land degradation and is a serious concern for global food security (IPBES 2018). FAO has projected that 90 percent of Earth's topsoil will be degraded by 2050 (FAO 2020), while also assessing in 2011 that food production need to increase by 70 percent until the same year to meet demands (FAO 2015). Furthermore, accelerated soil erosion can cause cascade effects such as losses of nutrients, carbon storage, biodiversity and soil and ecosystem resilience (Robinson et al. 2017). Increase in precipitation due to climate change is also projected to cause more severe soil erosion (O'Neal et al. 2005).

To mitigate erosion and its negative impact, global or regional strategies and policies such as United Nations' Sustainability Development Goals, and the European Commission's Common Agricultural Policy 2023-27 are attempting to address the issue (Panagos et al. 2020; Alewell et al. 2021; European Commission 2021). Meanwhile, within the field of landscape architecture, planning and management, soil erosion has become a strategic topic involving spatial risk assessment to indicate erosion hotspots within geographical areas (Guo et al. 2021), and to recommend subsequent preventionary measures such as increasing plant cover and developing ecological successions (Zuazo & Pleguezuelo 2009).

Starting in the 20th century there have been multiple attempts to development soil erosion models to estimate soil erosion from overland flow (Morgan 2005). According to Nearing (2013), such models mainly serves three purposes: a) to understand the extent of erosion within an area and trace changes over time (spatial risk assessment); b) to let land managers decide for preventionary measures; and c) as a basis for regulation recommendations to ensure management adherence. However, for soil erosion models to be effective tools in spatial risk assessment on a detailed landscape scale, and thus be relevant for local management, they need to reflect spatial hetereogeneity of erosion on that scale (Berberoglu et al. 2020). Additionally, preventionary measures are land cover specific, and cannot be upscaled as a general solution for a larger area of diverse land covers (Rickson 2014).

While soil erosion models are sometimes combined with a distributed hydrogical model (that simulates dispersed overland flow) to predict the distribution of erosion from overland flow on a detailed landscape scale, they greatly depend on the specific algorithm used to route that flow (eg., Mitasova et al. 2013). Flow algorithms of existing hydrological models are of different complexity (singular or multiple flow) and temporal resolution (for example monthly, or single rain events) (Borrelli et al. 2021). Meanwhile, dynamic triangular flow algorithms such as TFM-DYN are a relatively new type of multiple flow algorithm that simulate overland flow during rain events (Nilsson et al. 2022). They perform well compared to simpler single flow algorithms like the D8 algorithm in routing flow in a realistically distributed manner (Nilsson et al. 2022), but has to my knowledge never been used for soil erosion modelling of overland flow.

Furthermore, one existing soil erosion and deposition model that estimates soil erosion and deposition for rainfall events is the LImburg Soil Erosion Model (LISEM) (De Roo et al. 1996). It is a discrete numerical model specifically developed for spatio-temporal soil erosion estimation where space is subdivided into a grid within a geographical information system (GIS) (Jetten 2018). While LISEM seems to be using a less complex flow algorithm than TFM-DYN to route overland flow, its equations for erosion and deposition estimation may potentially intregate well in the latter since both models run simulations on a cell-by-cell basis in a GIS.

Stemming from this potential, in this study, a set of modified equations of LISEM are used to implement a soil erosion and soil deposition functionality into the dynamic triangular flow algorithm TFM-DYN. The algorithm is then tested by simulation of a single rain event.

1.2 Purpose, aim and goal

This study's purpose is to contribute to the on-going development of distributed soil erosion and deposition models for event-based rainfalls within the field of environmental modelling, and their application within the field of landscape architecture, planning and management, for example in spatial risk assessment at a detailed landscape scale. Based on existing theories and models of how soil is eroded and deposited, the study's aim is to understand how a mathematical soil erosion and deposition function can be implemented into a dynamic triangular flow algorithm, and, as a prototype, evaluate whether its logic is solid. Specifically, the primary goal of this mathematical function is to account for soil erosion, and its secondary goals are to account for how eroded sediment is transported and subsequently deposited.

1.3 Research questions

1. What are the benefits of using a dynamic triangular flow algorithm to model soil erosion, sediment transport through water, and soil deposition?

2. How can a mathematical function be added into a dynamic triangular flow algorithm to create a prototype soil erosion and deposition prediction functionality?

3. How can the logic of the resulting prototype soil erosion and deposition function be evaluated?

1.4 Limitations

Due to the vast scientific field and complex nature of soil erosion, this study limits its scope in modelling soil erosion regarding theory, existing models, geographical area, and time.

1.4.1 Soil erosion theory

The phenomena of soil erosion and deposition are quite complex and involve many interrelated processes and factors, both natural and anthropogenic (Morgan 2005). In this study some generalisations of factors that determine these processes are used, for example generalisations made by the LISEM model itself. The scope of this study excludes detailed biogeochemical aspects and other processes and factors that are interlinked with soil erosion (see e.g., Berhe et al 2018; Seeger 2024).

1.4.2 Soil erosion models

There are several types of models that aim to predict soil erosion (Borelli et al. 2021). While this study introduces the reader to soil erosion modelling in general, the focus is on using a set of equations introduced in LISEM and one distributed dynamic hydrological model (TFM-DYN).

1.4.3 Temporal limitation

Soil erosion is often estimated at an annual basis; however, the purpose of this study is to develop a soil erosion function for rain events simulated by a dynamic triangular flow algorithm.

1.4.4 Plant cover and prevention measures

While this study aims to model soil erosion based on fundamental soil erosion processes, its focus is primarily on erosive agents and soil characteristics. Even if plant cover and prevention measures play important parts in soil erosion (Zuazo & Pleguezuelo 2009), they will be generalised broadly and only covered briefly.

1.4.5 Soil erosion function evaluation and calibration

Since the purpose of this study is to develop and prototype a soil erosion function, I will not carry out an evaluation of the resulting model through for example sensitivity analysis, calibration or validation that are commonly used to assess environmental models (Bennett et al. 2013).

1.4.6 LISEM limitation

Although LISEM has several additional capabilities, such as calculating channel erosion (Jetten 2018), this study limits the use of the LISEM set of equations to calculating rainsplash and overland flow erosion.

2. Literature review

The purpose of the literature review is to give a theoretical foundation on which to base the development the soil erosion function. Literature, theories, and existing environmental models have been searched for through Google Scholar using key words such as: soil erosion, soil deposition, soil erosion model* and LISEM. The content mainly regards the disciplines of soil science, hydrology, and environmental modelling.

2.1 Fundamental soil erosion processes

The three parts in this section summarizes the three main factors influencing soil erosion according to Morgan (2005). Soil erosion refers to the planetary phenomenon of “erosive agents” (such as rainfall, wind, and gravity) breaking off soil particles from soil, and subsequently transporting them to other locations while there is enough kinetic energy. When there is not enough energy, the soil particles deposit in a new location.

2.1.1 Energy

According to Morgan (2005), potential energy and kinetic energy interplay to cause soil erosion. Potential energy refers to the difference in height between objects, for example the height difference between a falling raindrop and soil particles on the ground; as the raindrop falls the potential energy is converted into kinetic energy (Morgan 2005). The amount of kinetic energy of erosive agents, such as raindrops, runoff, and wind, determine how much erosive energy soil particles are exposed to (Morgan 2005). The amount of kinetic energy varies depending on the intensity of the rain and the volume and velocity of runoff (Morgan 2005).

2.1.2 Resistance

The properties of a soil can determine its resistance to erosion (its erodibility) (Morgan 2005). These properties include the soil’s composition, aggregate stability, shear strength, infiltration capacity (which can reduce the erosive agent of runoff) and organic and chemical content. (Morgan 2005). For example, clay particles' finer particle size binds them together by cohesive forces which makes them less erodible, while larger sand particles that lack this force more easily erode (Morgan 2005). At the same time, clay soils have a lower infiltration capacity than other soils due to smaller spaces between pores, which can lead to increased runoff and subsequent erosive energy (Morgan 2005).

2.1.3 Protection

Finally, different forms of plant cover can protect soil from being eroded. For example, the canopy of trees can intercept and delay rainfall which decreases the energy of the rain and runoff velocities (Morgan 2005). This aspect is largely determined by human land use in relation to vegetation (Morgan 2005).

2.2 Soil erosion and deposition caused by water

The following section describe different forms of erosion caused by surface water: rainsplash, overland flow (runoff), combined rainsplash and overland flow, rill and interrill, and gully erosion, and stream erosion. It also briefly details sediment (suspended soil) deposition. Since this study deals with soil erosion caused by surface water, I omit describing erosion related to wind, gravity, or subsurface water. It is important to note however that for example wind erosion has been shown to contribute third of total human-induced soil degradation whereas the rest was caused by water (Oldeman 1994, as cited in Morgan 2005).

2.2.1 Rainsplash erosion and crust formation

In the words of Morgan (2005), when raindrops splash on the ground an energy momentum is transferred to the soil particles. This momentum partly compacts the soil but also produces a "disruptive" force (Morgan 2005). This force stems from the behaviour of the water upon impact with the ground; the water is scattered and returned to its point of landing, which creates a local "sideways jet flow" (Morgan 2005). Raindrops typically fall with a velocity of 4-9 m/s and these local jet flow velocities are roughly twice of that magnitude (Morgan 2005). Soil particles can be propelled into the air by these jet flows and thereafter become suspended in droplets from the ruptured raindrop (Morgan 2005). Govers and Poesen (1988) point out that if the rainsplash occurs in a slope, the particles will further tend to eject downslope. When soil particles are loosened, Morgan continues, the soil aggregates are destroyed at the very top of the surface, forming a 0.1mm thick surface crust (Morgan 2005). The finer soil particles from these aggregates are pushed down and saturate pores in the soil aggregates immediately underneath them, causing a 1-3mm thick saturated layer underneath to form

(Morgan 2005). The saturated soil aggregates in this layer are more fragile and can easily crumble when struck again by raindrops (Morgan 2005). These soil particles can then be considered to have become initially eroded and will be more readily available for transport (Morgan 2005).

According to Foster (2013), most land surface soils are cohesive to various degrees. The consequence of soils being cohesive is that when erosion occurs during rainfall, it is not just particles of a particular size that are detached, but all smaller soil particles (smaller than gravel) (Foster 2013). Foster likens this with the illustrative example of hammering a concrete surface, where, upon impact, a variety of particle sizes are detached (Foster 2013). In a similar way, when rainfall hits the ground, it produces a variety of particle sizes to detach (see Fig. 1).

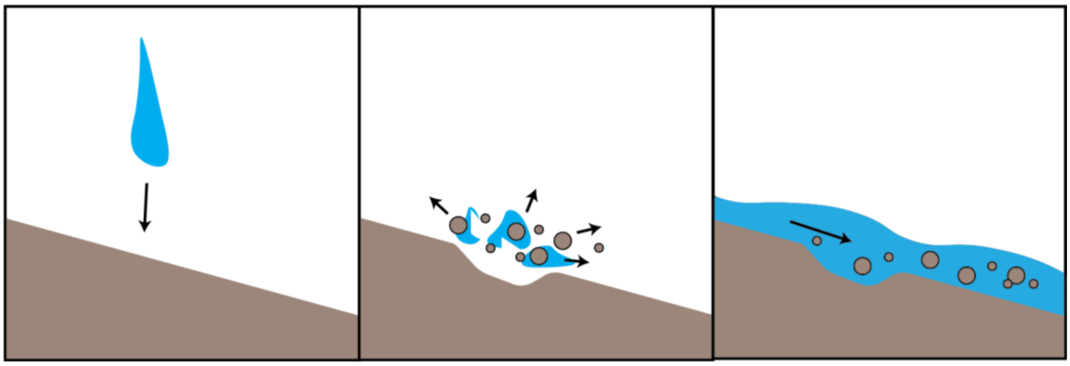

Figure 1. Time series of Foster's (2013) description of a raindrop's impact on ground that acts like a "hammer on concrete" to loosen and disperse locally soil particles of all sizes which are transported as overland flow once runoff velocity increases (except gravel or larger).

2.2.2 Overland flow

Morgan (2005) describes the characteristics of overland flow erosion when a soil's infiltration capacity is exceeded and the soil is saturated during a rainfall, it forces the water to flow overland and become runoff. This flow is rarely uniform in depth (i.e., "sheet") but more resembles tiny water courses without clearly defined routes. The flow is disrupted by and whirl about obstacles like rock and plant cover. The flow's kinetic (erosive) energy increases with turbulence. A turbulent flow consists of a complicated set of locally diverse eddies. Furthermore, the flow velocity is a key factor for eroding soil particles, since the greater the flow velocity the greater the flow's kinetic energy (Morgan 2005). They will therefore resist being eroded until a flow velocity threshold is reached (Morgan 2005).

In vegetated areas overland flow tends to be most common during saturated conditions, while in bare soil conditions overland flow may occur due to "Hortonian" conditions, meaning that the rainfall intensity exceeds the infiltration capacity without saturating the soil (Morgan 2005).

2.2.3 Combined rainsplash erosion and overland flow

When water depth in water puddles or overland flow increases during a rainfall event, it can strengthen splash erosion from additional rainfall (Palmer 1964, as cited in Morgan 2005). This is thought to be caused by the turbulence that the raindrops' kinetic energy passes on to the water (Morgan 2005) which disturbs the sheet flow (Zhang 2019). If water depth rises beyond a certain threshold, splash erosion decreases exponentially with increasing depth since the kinetic energy is dispersed in the water without affecting the ground surface (Morgan 2005). Experimentally, this threshold has been shown to equal the diameter of the raindrop or less (Palmer 1964; Torri & Sfalanga 1986; Mutchler & Young 1975, as cited in 2005). However, such splash erosion from turbulence has not been observed on sandy soils (Ghadiri & Payne 1979; Poesen 1981, as cited in Morgan 2005). Since water flow is typically greater during higher intensity rainfall events, rainsplash erosion are generally proportionally more impactful during lower intensity rainfall events (Jetten 2018).

2.2.4 Rill and interrill erosion

A rill refers to a small channel which is formed by soil erosion from overland flow (Morgan 2005). Rill erosion is therefore the erosion that occurs within a rill from concentrated flow of water (He et al. 2016). Meanwhile, interrill erosion occurs on surface areas between rills (Govers & Poesen 1988). When soil particles are detached from rainsplash erosion, they can either eject into nearby rills directly, or become suspended in overland flow that may also concentrate in rills (Govers & Poesen 1988).

The transformation of a water flow characteristic of overland flow to rill flow is considered to have four phases; during these phases the flow tend to change from a laminar "sheet" flow to a more turbulent flow (Merritt 1984):

- In the first phase the overland flow is relatively even (laminar) over a smooth soil surface, and erosion only occurs locally to single soil particles.
- In the second phase the flow has gone from being unconcentrated to having focused flow pathways in the ground, although the flow is still relatively laminar. The pathways cause the kinetic energy to drop due to an increase in surface roughness and eroding soil particles that "rolls" over the surface; over time, straight ripples appear in these pathways from the kinetic energy.
- In the third phase turbulence increases around ripples in the ground. At one point, a single ripple becomes bigger and more unsteady, creating greater local turbulence. This bigger ripple erodes the ground downstream which leads to the formation of a small and steep "headcut" and "plunge pool" in which more turbulence is created (Merritt 1984) by roll waves (Rauws 1987) and eddies (Savat & De Ploey 1982). As more particles are detached,

this headcut retreats upstream of this newly formed microrill (Merritt 1984).

- Finally, in the fourth phase the erosion rate becomes more constant depending on the transport capacity of runoff. As the headcut retreats upstream the microrill become wider and deeper by the flow, and more headcuts can be formed to further increase the size of the rill.

Rills can “migrate” both upstream and downstream (Morgan 2005). It occurs downstream depending on the flow’s shear stress and the soil’s strength (Savat et al. 1979), while it occurs upslope when developed headcuts retreat depending on the “cohesiveness of the soil, the height and angle of the headwall, the discharge and the velocity of the flow” (De Ploey 1989).

Once microchannels are formed however, they sometimes drain the runoff and then become filled by deposited soil particles from the upstream; whether a microchannel turns into a rill or is brief before it retracts depends on multiple factors (Quansah 1982; Dunne & Aubry 1986). Importantly, the formation of a rill needs enough focused water flow to raise the kinetic energy so that the channels get deeper and wider and can migrate upslope and downslope (Morgan 2005).

Rills seem to form more easily once the runoff crosses a threshold; on smooth or plane surfaces and for non-cohesive soils, a shear flow velocity of more than 3.0-3.5 m/s seems to increase sediment concentration more rapidly, and the flow can erode any loamy (sand, silt, clay) soil particle regardless of size (Govers 1985). According to Rauws and Govers (1988) the critical shear velocity for the formation of rills relates linearly to the shear strength of the soil.

2.2.5 Gully erosion

Compared to rills, gullies are rather long-lasting and mainly experience ephemeral flows during rain events (Morgan 2005). However, in contrast to river channels whose profiles usually are smooth and concave, gullies are abrupt pathways with several headcuts in a step-like manner (Heede 1975). Gullies also have greater depth-width ratio, behave more erratically and transport bigger amounts of sediments than stable channels (Morgan 2005). One standard definition to distinguish rills from gullies is that rills are smaller than 1m^2 in cross-sectional area (Poesen 1993). Gully formation is a sign of land instability and is typically only caused by accelerated erosion (Morgan 2005).

2.2.6 Stream erosion

Stream erosion occurs in river channels either on the banks or the bottom of the stream (Mitasova et al. 2013). The so-called Hjulström diagram was developed by Hjulström from studies on the river Fyrisån (Fig. 2). In 1956 the diagram was modified by Sundborg to also account for varying degrees of particle cohesion, and again in 1967 by Postma to account for compacted and non-compacted soils (Miedema 2013).

The diagram describes at what threshold velocities different particle sizes are eroded and deposited in a river at a 1m water depth. It also relates to the general trend in that increased particle size requires an increased rainfall energy to erode; the exception is for smaller clay particles where a decreased particle size requires greater velocity to erode due to the particle cohesion that clay particles manifest also in rivers (Fig. 2).

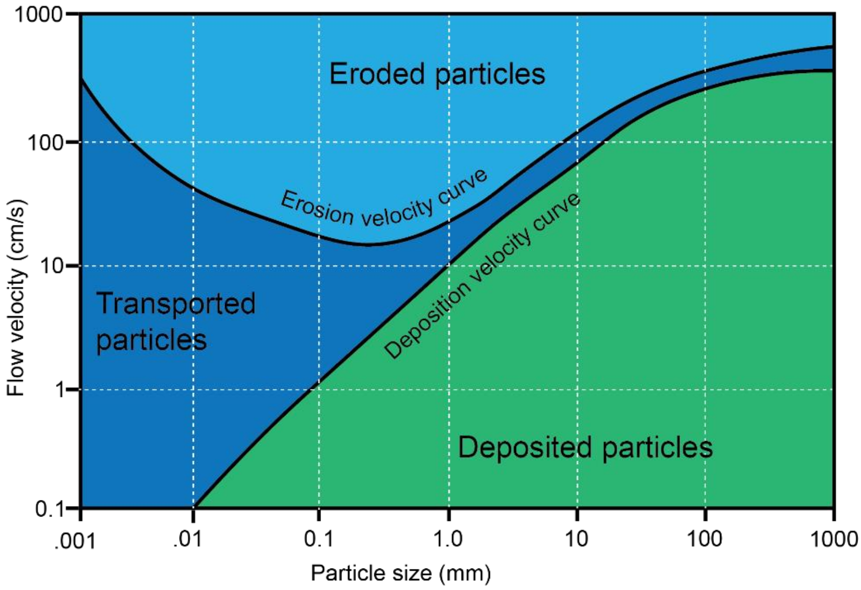

Figure 2. Hjulström-Sundborg diagram (1935; after Earle & Panchuk 2019). The diagram shows how flow velocities in streams required for erosion, transport or deposition depend on the particle size, where very large and very small (clay) particles require the greatest velocities for erosion. Meanwhile, clay due to their nimble size can be transported within a large range of velocities.

2.2.7 Sediment deposition

Deposition is caused when eroded soil particles (sediment) has been transported by water (such as runoff) and concentrate on a different location (Foster 2013). Soil particles remain suspended in water flow until the runoff's transport capacity is reached at which point deposition occurs (Haan et al. 1994, as cited in Mitasova 2013). Locally, particles tend to deposit within a few centimetres from the erosion origin in micro-depressions (i.e., surface roughness) (Foster 2013). Remote deposition refers to sediment that was carried over several metres or more and concentrate for example in low points in the landscape or in thick vegetation areas where flow decreases substantially (Foster 2013). Several equations for estimating the deposition rate (settling velocity) of sediment has been developed, for example one by Ferguson and Church (2004) which is based on Stokes' Law.

2.3 How soil erosion and deposition depend on soil properties

According to Morgan (2005), there are several different properties of soil that influence soil erosion and deposition, and they are often interrelated in a complex manner. These properties include aggregate stability, shear strength, infiltration capacity (which can reduce the erosive agent of runoff) and organic and chemical content. Fundamentally, these properties are determined by the composition of soil particles in a soil (Morgan 2005), which generally is divided into minerals, soil organic matter (SOM) and structural compounds of aggregates (Sparks 2003). In this section I will describe some broad characteristics of these particles and how they determine soil properties related to soil erosion.

2.3.1 Primary particles

Mineral soil particles (primary particles) include clay, silt, sand, gravel, and rocks and are distinguishable by their different sizes (Foster 2013). The size of a primary particle influences their chemical properties and consequently their tendency to erode from a soil. (Morgan 2005). Fig. 3 shows the range of sizes for different soil particles, including primary particles, and the kinetic energy required to erode them.

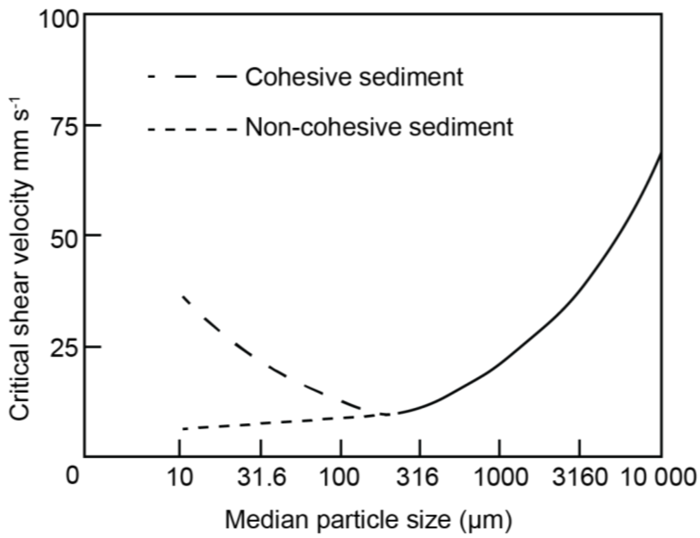

Figure 3. Critical shear velocity in turbulent water flow for soil particle detachment as a function of particle size (after Savat 1982 see Morgan 2005)

2.3.2 Soil organic matter, humus, and soil aggregates

Soil organic matter (SOM) is mainly developed from litter of plants (Lal 2021). The humus is formed through the presence of base minerals and SOM that bind together (Morgan 2005; Chapin et al. 2011). Soil aggregates are structural compounds of clay and humus and may also include silt and sand (Morgan 2005; Foster 2013).

2.3.3 Soil particle types and soil cohesion

Morgan (2005) explains soil cohesion as the interlinked behaviour of soil particles; the particles in a soil are normally connected with one another in relatively set positions. When a soil is exposed to shearing forces (gravity, shifting fluids and mechanical pressures) particles in the soil may glide over each other back and forth (Morgan 2005). In this process, the shearing forces are absorbed by contact between particles, cohesiveness of clay minerals and surface tension in unsaturated soils (Morgan 2005). A soil's general cohesiveness is related to the resilience of the particles to endure these shearing forces (Fig. 3). In the following sections I will describe a few aspects of how soil cohesion impacts soil particles' tendency to erode.

Crust formation

Section 2.2.1 describes how crust is formed during rainfall. However, the more clay and SOM a soil contains, its tendency to form crust lowers, due to its greater cohesiveness (Morgan 2005). Additionally, the formation of crust on the soil surface increases exponentially with cumulative rainfall energy (due to for example temporal length and intensity of the rainfall) (Govers & Poesen 1986), while infiltration capacity decreases exponentially (Boiffin & Monnier 1985).

Aggregates, SOM, and clay

SOM plays an important role in the cohesiveness of aggregates (Morgan 2005; Foster 2013). Most soils contain less than 15 percent SOM and sandy soils less than 2 percent (Morgan 2005), and soils containing less than 3.5 percent of SOM is typically susceptible to erosion (Evans 1980). However, there are exceptions where soils with very big amounts of SOM can erode easily and vice versa soils with very small amounts of SOM have a big resistance to erosion, which makes it difficult to generalise the erodibility for all soils (Morgan 2005).

Boix-Fayos et al. (2001) explain that the cohesion of aggregates depends on their size: aggregates larger than 10 mm are affected by the attachment and adhesiveness of plant roots; between 1 and 2 mm by the root and hyphae mesh; between 0.105-1.0 mm by SOM, roots, and hyphae; less than 0.105 mm by the mineral composition of clay and binding forces from microbial life.

Furthermore, earthworms contribute to more stable soil aggregates and higher hydraulic conductivity likely due to the higher amount of SOM in the soil that is the product of earthworm secretions (Glasstetter & Prasuhn 1992).

Moisture levels

According to Le Bissonnais (1990) there are three ways that a soil can react to rainfall depending on its moisture levels:

- Aggregates in dry soils break down rapidly if the rainfall intensity is high; The infiltration capacity decreases quickly as crust forms and can cause runoff even by low amounts of rain because there is no depression storage from uneven surfaces where water can fill.
- If the rainfall intensity is low, or if the aggregates already are moderately wet, the aggregates may break into microaggregates. While the surface becomes smoother, there are still big pores between the smaller aggregates so that high infiltration capacity is maintained.
- For initially saturated aggregates, the infiltration capacity is determined by the hydraulic conductivity of the soil in saturated conditions. Only soils with less than 15 percent clay, and low hydraulic conductivity, are susceptible to forming crust.

2.3.4 Soil erosion at different spatial scales

According to Morgan (2005), there are four different scales on which soil erosion can be considered differently:

- On a micro-scale (1 mm^2 to $1m^2$) the type of soil, land cover and slope are typically homogenous, so that erosion is mainly determined by the cohesion of soil aggregates. The levels of moisture, SOM soil fauna, especially earthworms, also contribute substantially. Furthermore, since the collapse of aggregates is largely caused by the kinetic energy of raindrops, the intensity and frequency of rain events also regulate the rate of soil erosion.
- On a plot scale (1 m^2 to $100m^2$) erosion is determined by runoff and the causes of it, such as the soil's infiltration capacity and micro-topography. The arrangement of areas that are crusted and non-crusted or bare and covered by vegetation will decide where runoff is formed and how it moves and collects sediment. If the slope is steep enough or the soil is very erodible rills may form, but otherwise lesser interrills are more common.
- On a field scale (100 m^2 to $1000m^2$) overland flow is typically directed towards low areas. However, the amount of interrill erosion can vary depending on the rainfall intensity which means that the contributing area of runoff can differ.
- On a catchment scale (>$10000m^2$) there are usually different areas that are characterised by different types of erosion. Some areas may be more affected by rainsplash erosion, while others are more exposed to interrill erosion, and yet others by rill erosion, and finally those by gully erosion.

Obstacles such field boundaries, roads and natural topography contribute to the formation of runoff pathways. According to Chapin (2011), erosion mostly occurs on steep slopes and deposition in valleys and depressions.

2.4 Environmental modelling

This section starts by describing what models and environmental modelling are, and then addresses distributed hydrological models and finally models for estimating soil erosion.

Wainwright and Mulligan (2012) describe models and environmental modelling in-depth: in essence, a model is generalization of reality, and reality can be understood as several complex and interlinked processes that often are hard or impossible to observe yet which produce certain effects and results. A model is based on knowledge of these processes, and the parameters that determine them, and can be tested to see if the effects can be repeated (Wainwright & Mulligan 2012). Furthermore, models are helpful in simplifying these processes so that they become more comprehendible (Wainwright & Mulligan 2012).

According to Wainwright and Mulligan (2012), the ideal model is *parsimonious*, meaning it reflects reality's complexity with a minimum number of necessary parameters. This is partly because it is costly to gather data about a complex system (for example by collecting field data), and partly because the outcome of simple models often more accurately resembles the measured field data than complex models (Wainwright & Mulligan 2012). Yet a model that is too simple will fail to be realistic; one of the main challenges in developing a model is striking a balance between simplicity and complexity (Marsh & Hau 1996).

In a similar manner, environmental models generalize real environments, and account for the interplay between several interconnected complex environmental systems (biotic and abiotic) across time and space (Wainwright & Mulligan 2012). When they are used to understand consequences of future events, for example climate change, they only serve as projections into the future, rather than predictions, since they are only based on the currently available knowledge (Wainwright & Mulligan 2012). Therefore, one should be careful in drawing conclusions based on the output of the model (Wainwright & Mulligan 2012).

Environmental modelling is also useful as a supplement to field measurements of environmental variables. While field measurements can provide accurate point data, models can generalise these measurements, or combine them with other available environmental data to estimate environmental variables at other points in time and for spatially hetereogeneous land covers (Pianosi 2014). Models can also in this way consider changes in environmental data and to predict changes in environmental variables, their impact, as well as suggest management actions (Pianosi 2014).

The process of environmental modelling includes data collection and measurement, parameterisation, and model structure development (Wainwright & Mulligan 2012). A model structure usually consists of numerical parameters and variables embedded in mathematical equations or algorithm; an equation can help reduce the complexity of a system into a set of variables (Wainwright & Mulligan 2012). By adjusting these one at a time one can experiment with their respective impact (Wainwright & Mulligan 2012). Furthermore, calibration of parameters and validation of the model output is typically carried out to determine the accuracy of the model (Wainwright & Mulligan 2012).

2.5 Hydrological models

Hydrological models are environmental models that model planetary flows of water, for example overland flow caused by rainfall (Bobba et al. 2001). Hydrological models can be considered to be on a spectrum of process complexity, i.e., how complex their modelling of hydrological processes are, where conceptual and empirical models can be considered less complex than process-based and physical models (Fatichi et al. 2016; Clark et al. 2017; Enemark et al. 2019). Particularly complex, physical models can consider a myriad of hydrological and biophysical processes such as the influences of snow melt and evapotranspiration (Archfield et al. 2015). In the case of models of overland flow, they can also be considered complex in terms of how much they model hydrological processes in relation to details of the landscape that affect the lateral flow of water, i.e., spatial complexity (Clark et al. 2017), where lumped and semi-distributed models are less complex than distributed models (Archfield et al. 2015; Okiria et al. 2022).

2.6 Distributed hydrological models

This section aims to describe distributed hydrological models in general, and then addresses triangular irregular network (TIN) models and specifically the TFM-DYN model.

Yun et al. (2022) describe distributed hydrological models as numerical models that compute runoff based on topographical approximations usually in the form of a digital elevation model (DEM). A DEM divides a continuous terrain surface, such as a watershed, into a grid of cells where for each cell a flow of mass is calculated (2022). In other words, a cell serves as a *flow domain*, e.g., a discrete areal unit of flow in the model (Yun et al. 2022). The occurrence of distributed hydrological models has increased in the late decades due to greater computational capabilities (Wainwright & Mulligan 2012). However, distributed models have weaknesses such as difficulties in parameter estimation and quantifying uncertainty (see e.g., Beven 2001, Zhou & Liu 2002, Archfield et al. 2015). Nonetheless, they are often considered valuable where understanding of the complexities of flow processes and their spatial distribution are necessary such as in a watershed where the conditions are inherently complex and heterogeneous (Fatichi et al. 2016; Clark et al. 2017). In other words, a parsimonious distributed hydrological model will necessarily account for greater complexity than for example a conceptual hydrological model (Fatichi et al. 2016).

2.6.1 Single flow direction (SFD) and multiple flow direction (MFD) algorithms

Fundamentally, a distributed hydrological model based on a DEM uses algorithms that either calculates a singular flow direction (SFD) or multiple flow direction (MFD) between flow domains (Yun et al. 2022). It means that a SFD algorithm can transport the flow mass from one cell to a neighbouring cell, while an MFD algorithm can distribute the same mass to multiple neighbouring cells (Yun et al. 2022). Because of this MFD algorithms are considered to describe flow more accurately than SFD algorithms (Zhou & Liu 2002; Wilson et al. 2008); the visual result of SFD algorithms appear as relatively straight and unnatural lines, while that of MFD algorithms tend to resemble a complex network of flow paths (Seibert and McGlynn 2007). SFD algorithms often produce unrealistic flow routes, especially for surfaces where flow typically diverges such as for mathematical plane or horizontally convex surfaces (Pilesjö & Hasan 2014).

2.6.2 Triangular irregular network (TIN) multiple flow models

A triangular irregular network multiple flow model uses a specific type of MFD algorithm based on a triangular irregular network (TIN) (Seibert & McGlynn 2007). The TIN is created from the height data of the DEM (see Fig. 4). In comparison to a DEM, a TIN also works as a representation of elevation but can be used differently (Wilson et al. 2008). In a TIN, the midpoint of each cell and its neighbouring eight cells is connected by triangles called facets (see Fig. 5). These facets have a horizontal and vertical dimension and divide each cell in the DEM (Pilesjö & Hasan 2014). In combination with the DEM, they enable the computation of water mass flow (Seibert & McGlynn 2007; Yun et al. 2022).

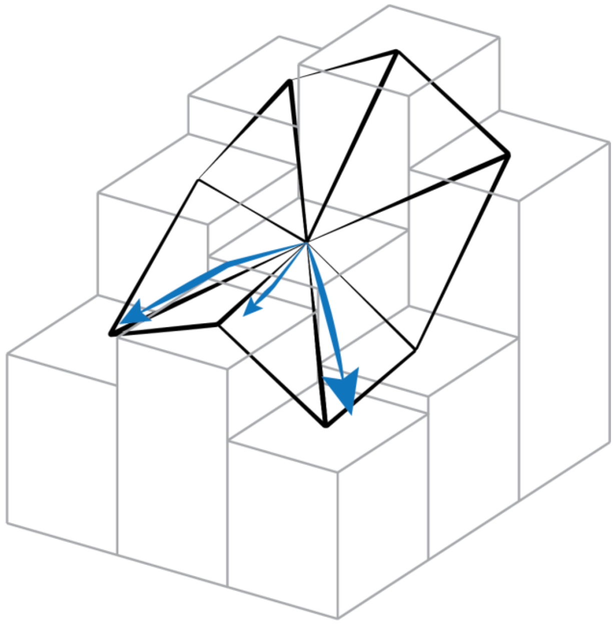

Figure 4. A TIN with triangular facets (black) based on a 3x3 DEM (grey) calculating a multidirectional flow (blue) from the central cell (after Seibert & McGlynn 2007)

2.6.3 The TFM model

The TFM model is an example of a MFD algorithm that uses a TIN to calculate surface water flow distribution and flow accumulation (Pilesjö & Hasan 2014). This is exemplified in Fig. 5 that shows how each facet's plane is calculated in the TIN.

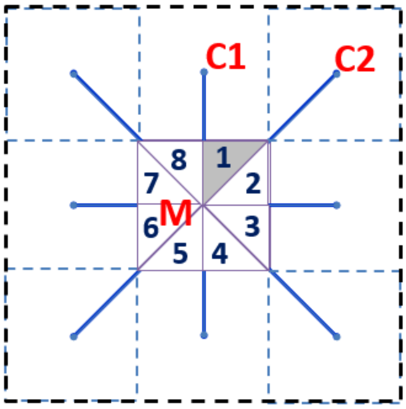

Figure 5. The TFM divides each cell into eight facets, each of which are planes formed by three cell centers and their respective elevation. For example, Facet 1 is formed by calculating the center points of cell M, C1 and C2. (Nilsson et al. 2022).

As shown in Fig. 6, the water flow from each facet in TFM can either be directed immediately to a neighbouring cell (*1*), or to a neighbouring facet (*3*), or be divided and sent to either two facets (*4*) or a facet and a neighbouring cell (2). The use of facets has shown to improve distributed routing calculations compared to eight other flow algorithms, for example the D8 algorithm (Pilesjö & Hasan 2014). The D8 algorithm is a SFD algorithm that only routes flow from one cell to another resulting in a flow connectivity the width of a single cell (see Section 2.6.1). Comparatively TFM can route flow to multiple cells as well as within each facet in a cell. The latter is helpful as it redistributes flow within the cell before leaving the outlet facet, thus allowing for the cell's internal elevation structure (facets) to also influence the flow direction (Pilesjö & Hasan 2014).

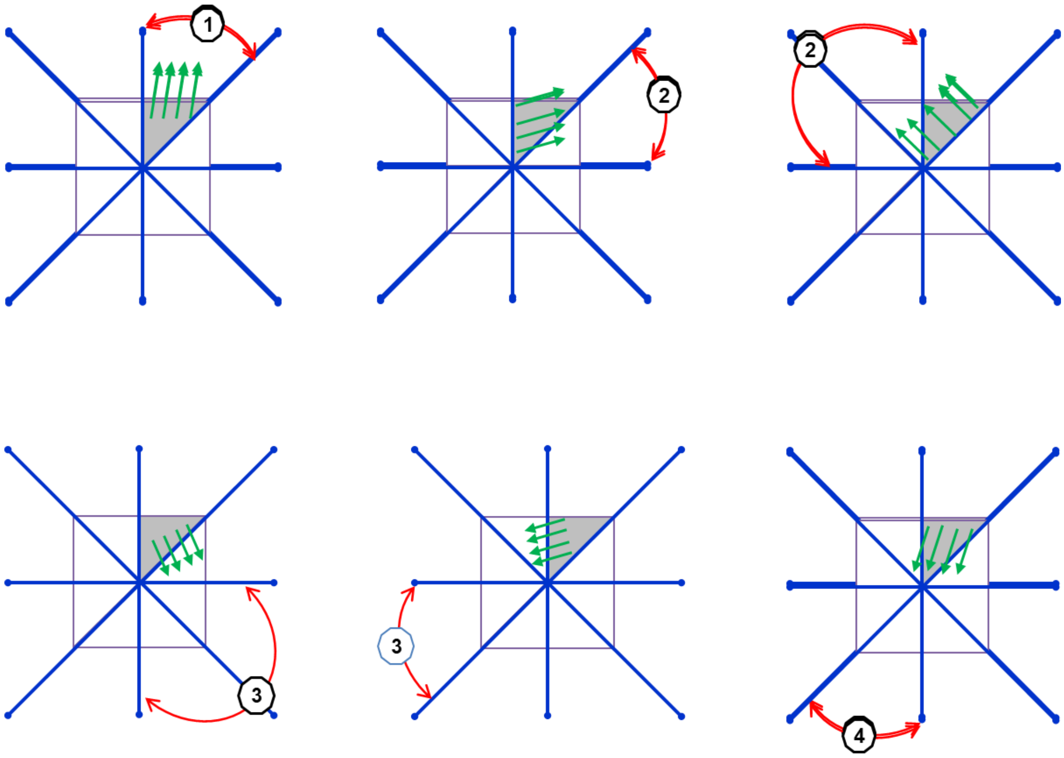

Figure 6. An illustration of how water can be routed from one triangular facet to other facets. Different aspect values lead to different actions (Pilesjö & Hasan 2014)

2.6.4 The TFM-DYN model

The aim of this study is to add a soil erosion and deposition prediction functionality into TFM-DYN (Fig. 7). In addition to using the flow routing algorithm of TFM, TFM-DYN adds the ability to dynamically route flow depending on the water depth (see Figure 8a & 8b). As such, it is suitable for simulating rainfall events and subsequent overland runoff where water depth can change dynamically depending on change in environmental variables such as the infiltration conductivity of a soil (Nilsson et al. 2022). The model inputs a DEM to create a TIN, and also inputs infiltration capacity, surface friction, precipitation in each cell and inlets and outlets (underground storm water network) (Nilsson et al. 2022).

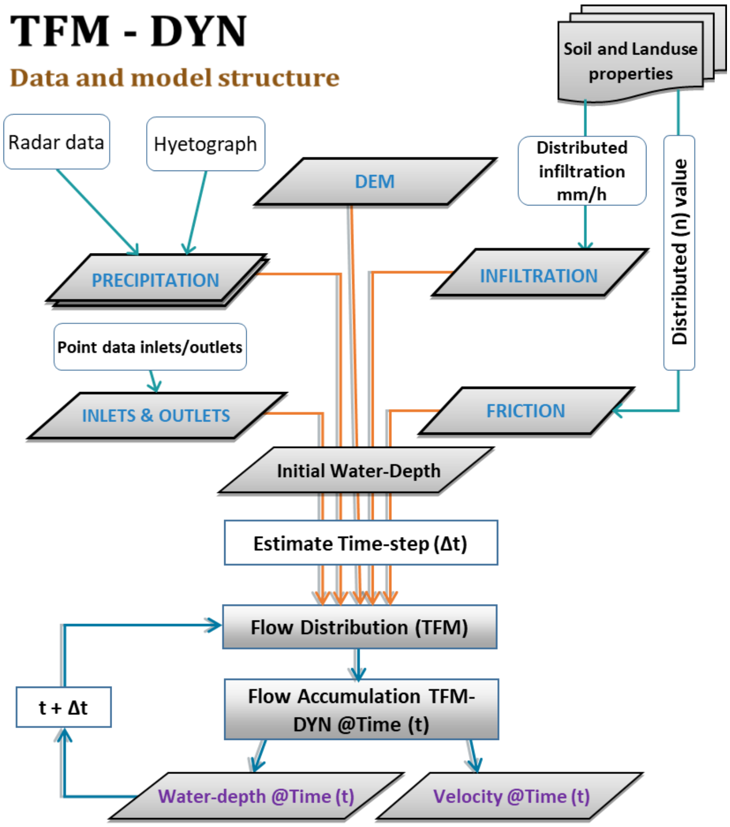

Figure 7. A conceptual diagram to explain the model sequence and input data of TFM-DYN (Nilsson et al. 2022)

Once the simulation starts in TFM-DYN, runoff flow is calculated for each time step in each cell using the facets in the TIN (Nilsson et al. 2022). The output includes water velocity and water depth for each cell and time step. It can also calculate slope in radians, upstream contributing area (flow accumulation) (Nilsson et al. 2022). In the model, the height data is dynamic (Fig 8a-b), in the sense that it continuously adds the accumulated water depth on a cell to the DEM (Nilsson et al. 2022). For example, runoff directed to a depression in the ground may cause it to fill, since the DEM is updated by water depth in the hole in each time step (Nilsson et al. 2022). Once the hole is filled additional runoff may be directed elsewhere to the new low height cells (Nilsson et al. 2022).

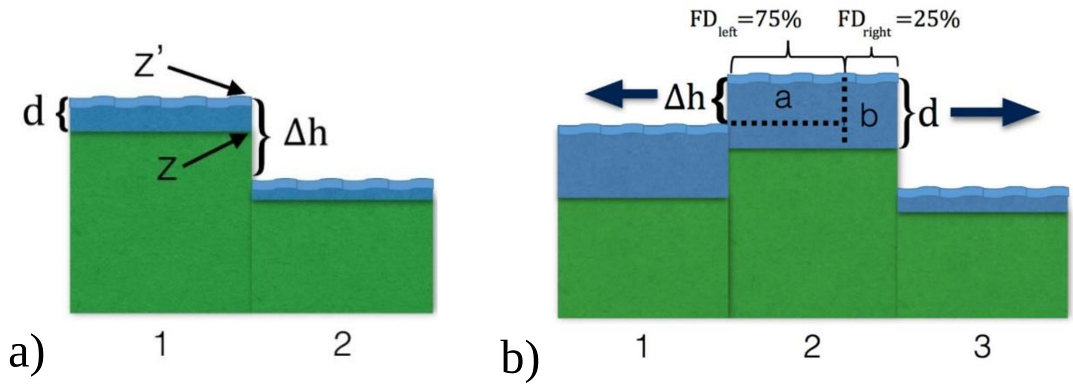

Figure 8a & 8b. 8a shows how water will be routed from cell 1 to the downstream cell 2 in TFM-DYN. The d is water depth, z is ground elevation, z' is water surface elevation and delta-h is the height difference between the two cells' water surface elevations. Meanwhile, 8b shows how, from cell 2, maximum 75% of water will be routed to the left, and maximum 25% to the right. Delta-h is smaller between cell 2 and cell 1, which could restrict the available water to be routed left compared to in cell 3, where the restricting factor instead is the water depth. However, due to the TFM algorithm and its use of facets, water can still be routed to the left. This illustrates how flow routing dynamically depends both on water depth and the TFM algorithm in each cell. (Nilsson et al. 2022).

2.7 Soil erosion modelling

Similarly to hydrological models, soil erosion models are often categorised as either empirical, conceptual, physical, or process-oriented models (Borrelli et al. 2021), as well as lumped, semi-distributed or distributed models (Lenhard et al. 2005). Since this study focuses heavily on the usage of the physically based LISEM set of equations for soil erosion and deposition, I will in this section first introduce what a physical model is, as well as lumped, semi-distributed and distributed models. I will then elaborate further on LISEM. Lastly, I will identify some gaps in soil erosion modelling.

2.7.1 Lumped, semi-distributed and distributed soil erosion models

As explained by Lenhard et al. (2005), a lumped model treats the whole area for soil erosion estimation homogeneously. If the area is a watershed, the input parameters regarding hillslope (topography), soil properties and rainfall are treated uniformly. One such lumped conceptual model is the sediment delivery ratio (SDR) which is the ratio of sediment at the watershed outlet to the overall soil erosion within the watershed (Lenhard et al. 2005). A lumped model's homogenous generalisation of the landscape can produce erroneous results; in the case of SDR the sediment delivery may be estimated to be great if the landscape is convex rather than concave (Lenhard et al. 2005). However oftentimes the total amount of estimated eroded soil can be similar between lumped and distributed models, and it can therefore be motivated to use such a model due to its ease of use (Jetten et al. 2003).

There are also semi-distributed (semi-lumped) models which divide the watershed into different subbasins (Lenhard et al. 2005). SWAT (Arnold et al., 1998) and HYPE (Lindström et al. 2010) are two examples of such models. However, the division into subbasins is relatively arbitrary (Lenhard et al. 2005), and within each subbasin the landscape is still treated homogeneously (see e.g., Fistikoglu & Harmancioglu 2002).

In comparison, a distributed model is helpful to distinguish where in the landscape soil erosion occurs (Jetten et al. 2003). It only treats the landscape homogeneously within the cell resolution (see e.g., Panagos et al. 2015; Aiello 2015; Wang et al. 2023).

2.7.2 Physical soil erosion models

Physical soil erosion models are models that typically try to understand the physics behind the detachment of soil particles and their subsequent transport in and deposition from hydrological flows (see e.g., Pandey et al. 2016). There are many different physical soil erosion models that are either lumped or distributed, or event-based or continuous (Pandey et al. 2016). Due to the nature of soil erosion largely being caused by water, physical models often depend on a hydrological model that simulates water flow (Pandey et al. 2016).

Physical models can be contrasted to empirical models. Most empirical models, such as the lumped USLE model, use measurements of soil loss from erosion plots (Dotterweich 2013). An erosion plot is an area where artificial runoff is poured from an upslope area and then collected and measured (Kinnell 2017). The output is usually mass per unit of time (Batista et al. 2019). However, a criticism of empirical models is that they often do not consider scale dependency (Parson et al 2009). Physically based models become useful when estimating erosion for topographically and soil-relatively complex and spatially large landscapes because it is simply difficult to empirically measure erosion for such conditions (Pandey et al. 2016). They are also considered better at more accurately extrapolating erosion estimation for different land uses and to simulate erosion and deposition processes for single rainfall events (Pandey et al. 2016). In terms of downsides, physical models often require large datasets, can be difficult to use, and may lack good validifying measurements or clearly conveyed shortcomings (Pandey et al. 2016).

2.7.3 The LISEM model

LISEM is a physically based model published in 1996 as a planning and conservation tool by estimating distributed soil erosion from single rainfall events for small catchment areas (De Roo et al. 1996). As a discrete model, it was one of the first soil erosion models to divide space into a grid of cells and time into time steps within a geographical information system (GIS) (De Roo et al. 1996; Borrelli et al. 2021). This allowed the model to account for the spatial variability of erosion within a watershed regardless of its different spatial features (Borrelli et al. 2021). Interestingly, it has been shown to be more flexible for usage in various spatial resolution sizes than at least one other distributed soil model (Starkloff & Stolte 2014). Essentially, therefore, it can be used for predicting erosion at a varyingly detailed scale, typically ranging from micro to plot scale as mentioned in Section 2.3.4. It also enables it to capture the spatial heterogeneity within a watershed, such as differences in soil cohesion and plant cover among different land cover types, that may influence the levels of soil erosion differently during a rain event (De Roo et al. 1996).

In terms of water flow, LISEM deals with both vertical flow through multiple soil layers and lateral overland flow (Jetten 2018). It also considers different soil conditions such as level of wetness and compactness (Jetten 2018). It uses several shallow flow equations to simulate overland flow, channel flow and flooding, such as an equation for kinematic flow derived from the conservation of mass and Saint-Venants equations (Jetten 2018). The output of these equations are then used for calculating overland flow erosion, rainsplash erosion and sediment deposition (2018). To distribute the suspended sediment across a grid-based area, the model uses a local drainage area (Jetten 2018). It considers overland flow erosion only as rill erosion because it is significantly greater than sheet erosion (Herweg 1996; Jetten 2018).

Soil erosion and deposition in LISEM is calculated through a set of equations which are covered in detail in Section 3.3. In summary, the balance in erosion and deposition is equal to the sum of two types of erosion (splash detachment Ds and overland flow detachments Df) minus sediment deposition:

$$e = Ds + Df - Dp \tag{1}$$

where:
e = balance of continuously counteracting erosion and deposition [kg m^{-2} s^{-1}]
Ds = splash detachment [kg m^{-2} s^{-1}]
Df = overland flow detachment [kg m^{-2} s^{-1}]
Dp = sediment deposition [kg m^{-2} s^{-1}]
(Starkloff & Stolte 2014).

2.7.4 Gaps in soil erosion and deposition modelling

While many physical soil erosion models use hydrological components to transport eroded sediment (Pandey et al. 2016; Epple et al. 2022), to my knowledge, no studies have used a dynamic triangular flow algorithm for this purpose and for a single rainfall event. In this section, I address some gaps in soil erosion modelling that could be filled by including a soil erosion and deposition function in an MFD-algorithm like TFM-DYN.

Currently, the most common model to predict soil erosion is the empirical USLE family of equations, even if physically-based and distributed models such as LISEM are becoming used more frequently (Borrelli et al. 2021). As such, a lumped model like USLE influences to a greater degree decision-making around soil erosion than physically based models, resulting in a gap of understanding of the utility of the latter (Borrelli et al. 2021). Also, as mentioned in Section 2.7.1, while USLE can offer insight on soil erosion on a large scale, it cannot model distributed soil erosion within a watershed. Using such a model, we do not fully know what is happening within the landscape in terms of erosion as they lack simulation of sediment movement and deposition (sedimentation) (Alewell et al. 2019).

Soil erosion models have been developed in an effort to estimate and visualize soil erosion for watersheds, and also to address knowledge gaps in closely related issues such as climate change and carbon mitigation, and hydrology and flood prediction (Alewell et al. 2019). However, without understanding the distribution of erosion, sediment transport and deposition on a detailed landscape scale, it is difficult to use the model for detailed applied analysis in the field of landscape architecture, planning and management. This includes for example how to recommend land managers where to invest in effective preventionary measures Nearing (2013).

Meanwhile, physically-based distributed models depend greatly on their different flow routing algorithms (Epple et al. 2022) and as such can vary in the degree to which flow is routed in a distributed manner. For example, LISEM uses a relatively simplistic local drain direction map (see e.g., Rahmati et al. 2013) which is sensitive to local depressions (UTwente, n.d. -a). Also, Epple et al. (2022) mentions several other physically based models which use relatively simplistic D8 flow routing algorithms. As such, another gap of understanding could be what the implications would be of increased usage of soil erosion models that utilise routing algorithms that increases the level of local spatial distribution beyond simplistic D8 routing algorithms. The benefits of such increased local detail could be beneficial for local erosion prevention and local erosion policy-making due to an increased awareness of where soil erodes and deposits locally, and what the main contributing factors are at that location (Epple et al. 2022).

Since dynamic distributed MFD algorithms like TFM-DYN can simulate water depth and surface flow dynamically and in high resolution, there is a potential to, in a corresponding manner, trace the spatial distribution of erosion, sediment transport, and deposition in great local detail. Combined with erosion equations from LISEM that, as already mentioned, are flexible in terms of use for high resolution (Starkloff & Stolte 2014), TFM-DYN could assist in filling the gap of understanding the benefits of high-resolution dynamically distributed modelling of soil erosion and deposition. An implemented soil erosion and deposition function in TFM-DYN could help to, for example, more accurately recommend land managers specific locations (on a field, plot or micro scale) within a watershed that could be the most positively impactful when introducing preventionary measures. Such a measure could be to increase plant cover that mitigates erosion, and to optimise this measure for the particular local conditions (by for example selecting plant cover species that are best adapted for local soil conditions) (Nearing 2013).

3. Method

This section describes the study's method. The onset has been deductive. A deductive onset means to base one's work on existing theoretical knowledge to come up with ideas that can be tested empirically (Clark et al. 2021). The collected materials from the literature overview are used in the latter step of environmental modelling. Fig. 9 provides a conceptual description of the steps in the process.

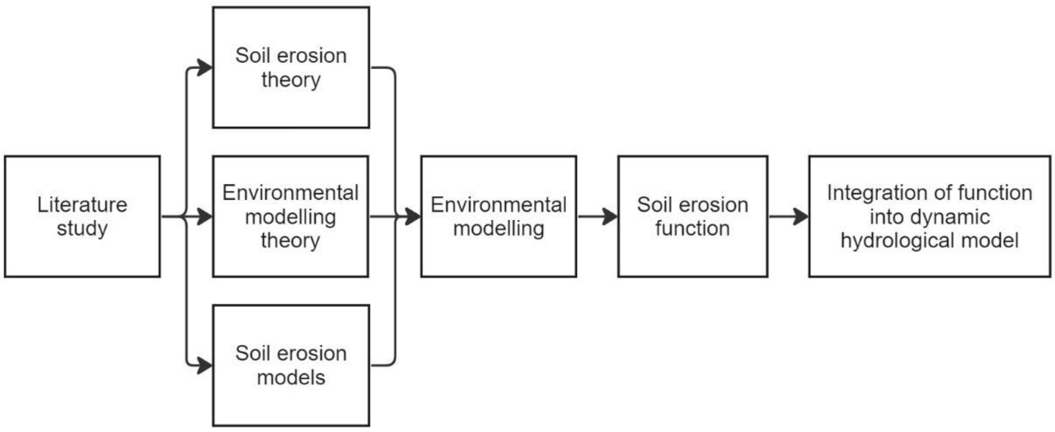

Figure 9. Methodological overview for the development of the soil erosion and deposition function

3.1 Environmental modelling for implementing a soil erosion and deposition function in a dynamic hydrological model

Environmental modelling is carried out to simplify and numerically estimate the real-world phenomenon of soil erosion by adding a numerical soil erosion and deposition function into an existing dynamic hydrological model (TFM-DYN). Data collection and model structure development are carried out as parts of the environmental modelling process. The model structure development is based on iteratively creating prototypes of the soil erosion and deposition function, and for each iteration investigate its performance (Wainwright & Mulligan 2012).

3.1.1 Conceptual model of soil erosion model LISEM added into dynamic flow algorithm TFM-DYN

The added soil erosion and deposition functionality of LISEM in the dynamic hydrological TFM-DYN model is shown in Fig. 10. The aim is to use TFM-DYN's dynamic MFD algorithm, and the water velocity and depth for each cell in each time step that it calculates. Several output variables from TFM-DYN are used, including water velocity, water depth, flow accumulation, and the proportion of water *wp* that leaves every cell in each time step.

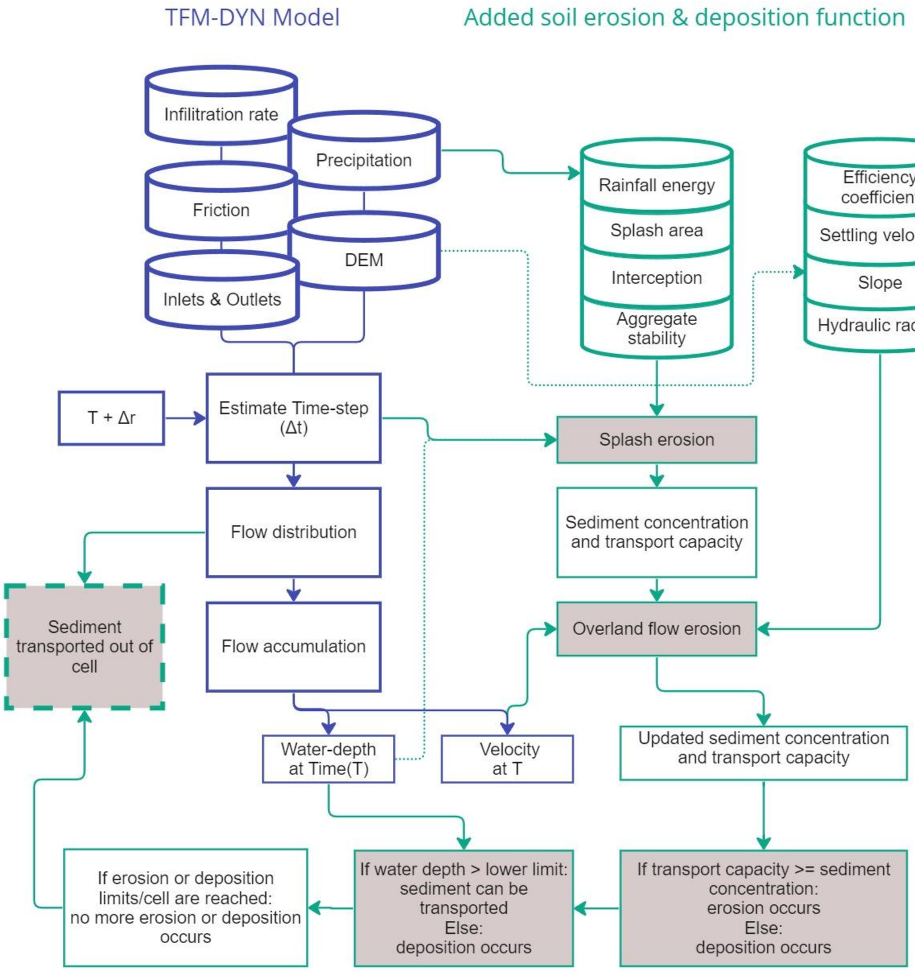

Figure 10. Conceptual diagram of soil erosion and deposition function inspired by LISEM added to the TFM-DYN model. Items in green are the new added functionality to simulate soil erosion and deposition. Items filled with brown are key steps in the function. For example, the key step of calculating Splash Erosion involves the input data of splash area, plant height, interception, aggregate stability, and rainfall energy based on the precipitation data from the TFM-DYN as well as the time step length. Meanwhile, the bottom boxes show different conditions for where erosion or deposition can occur. See Section 3.2 for a complete breakdown of all steps.

3.1.2 Input data preparation

The input data to the soil erosion function and how they were obtained are described in Section 3.4. The input data were prepared using the GIS-software ArcGIS Pro (ESRI 2011).

3.1.3 Object-oriented programming

The soil erosion function was added into TFM-DYN using object-oriented programming in the programming language Python (Python Software Foundation) using the integrated development environment (IDE) PyCharm (JetBrains 2023). Apart from the base program the library NumPy was used (Harris, Millman & van der Walt). TFM-DYN was then run, and the results were exported for further processing.

3.1.4 Output data processing and visualisation

The results of the soil erosion function are in formats of tables, maps, and 3D-models. I used Python (Python Software Foundation), the Pandas library (McKinney 2010), PyCharm (JetBrains 2023), Microsoft Excel (Microsoft Corporation 2018), Google Colaboratory (Google 2024) and ArcGIS Pro (ESRI 2011) to process the model output.

3.1.5 Model classification

The soil erosion and deposition function has been developed with the intention to account both for erosion and deposition heterogeneously within the landscape. The function can be considered a hybrid model in the sense that it nests a set of LISEM equations within TFM-DYN.

3.2 Soil erosion and deposition function

This section describes in a chronological order the different steps of the soil erosion and deposition function that occur in each cell and time step during the TFM-DYN simulation of the rain event. Fig. 11 illustrates these steps altogether. For clarity, when the word sediment is used in this section it refers to sediment that is suspended in water from rainsplash or overland flow erosion unless otherwise stated (i.e., “deposited sediment”).

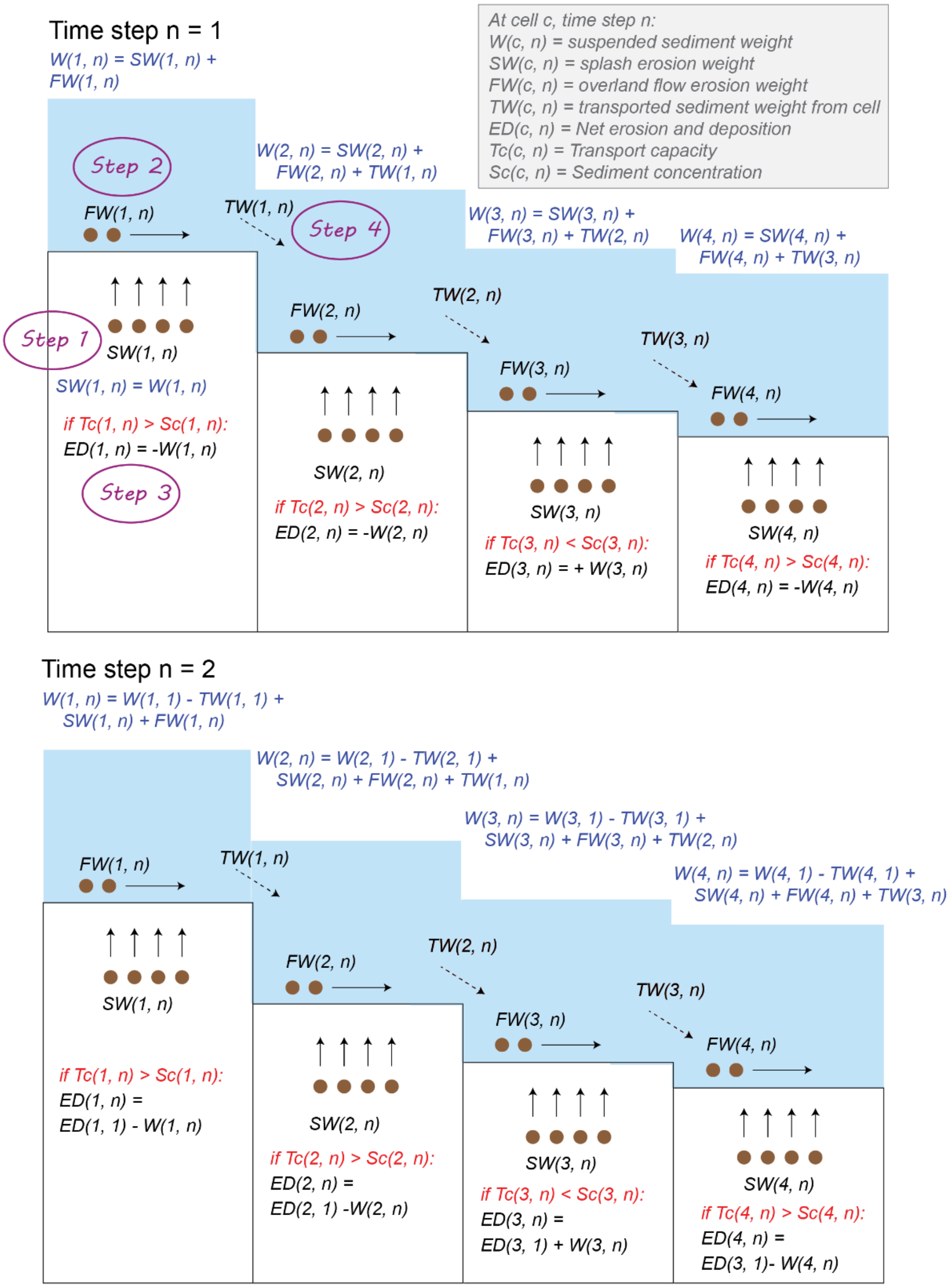

Figure 11. Cell-to-cell example of particle flow. Step 1 calculates splash erosion, step 2 overland flow erosion, step 3 determines where deposition occurs, and step 4 distributes sediment in flow direction.

3.2.1 Step 1: Calculate splash erosion

At the start of a given time step in the TFM-DYN simulation, the soil erosion and deposition function use a set of equations and their variables from LISEM to calculate a mass of soil particles that detaches from the ground due to the impact of rainfall in each cell where precipitation occurs and forms suspended sediment. This sediment mass (kg) represents the local splash erosion within each cell in the simulation. The sediment mass is dynamic for each time step and cell because the LISEM variables that are used to generate the mass can change values depending on the values of the output variables that TFM-DYN produces in each time step and cell (see Fig. 7; Section 3.3). For example, splash erosion will decrease exponentially as water depth increases.

The sediment mass from splash erosion is summed with any existing mass of sediment that was transported into the cell during the previous time step (see Step 4). Importantly, if there is already deposited mass of sediment that settled during earlier time steps, the deposited mass is subtracted by the new mass of splash erosion. This allows for re-suspension of already deposited soil mass in any time step and cell.

3.2.2 Step 2: Calculate overland flow erosion

After step 1, the existing mass of suspended sediment in each cell is used to derive suspended sediment concentration (kg m^{-3}) in each cell. This concentration is used to determine overland flow erosion according to another set of LISEM equations and TFM-DYN output variables (see Section 3.3). Just like for splash erosion, the overland flow erosion results in an additional suspended sediment mass which is subtracted from any already existing deposited soil mass in the cell. This sediment mass is summed with the existing mass of suspended sediment in each cell, and finally sediment concentration is derived from it. Now the suspended sediment concentration reflects the addition of sediment mass in the cell from splash erosion of step 1, overland flow erosion of step 2, as well as sediment that was transported into the cell in the previous time step (see Step 4).

3.2.3 Step 3: Determine where deposition occurs

At this point, the function will determine whether the sediment mass present in each cell will deposit or not in its cell. Deposition of the sediment mass occurs in the cells where suspended sediment concentration is greater than the transport capacity of that cell as calculated by the set of LISEM equations and TFM-DYN output variables (see Section 3.3). If the transport capacity is less than sediment concentration, the water flow is considered not to have enough momentum to transport the whole sediment mass to other cells; the flow will only transport the sediment equivalent to its transport capacity. In cells where sediment concentration is greater than transport capacity, the sediment mass available for deposition corresponds to the difference between sediment concentration and transport capacity. The rate at which deposition occurs is described in Section 3.3.3.

3.2.4 Step 4: Flow distribution of suspended sediment

The last action of the soil erosion and deposition function in each time step is that the sediment mass in each cell is distributed in the same proportion as water is distributed according to the dynamic triangular flow algorithm of TFM-DYN. Therefore, some sediment mass will stay in the cell if there is not enough velocity or time to transport all water out of the cell. This mass will be still treated as suspended in water and considered as part of the existing sediment mass already present in the cell (as mentioned in Part 3). Meanwhile, the mass that is distributed to other cells now is added to the existing sediment mass of those cells.

3.2.5 Main output of soil erosion and deposition function

The main output of the soil erosion and deposition is Net Erosion/Deposition (see Fig. 11). For example, if Net Erosion/Deposition at a given cell and time step is positive, it means that up until that point in time, more soil mass (kg) has been deposited in that cell than has been eroded from that cell. Vice versa, if the value is negative, more soil mass has eroded. If the value is 0, equal amount of soil mass has eroded and deposited, or neither have occurred. Additionally, Net Erosion is a supplementary output to Net Erosion/Deposition, as it only tracks how much erosion has occurred at a given time step and cell.

3.2.6 Erosion and deposition limits

The soil erosion and deposition function features a set weight limit to the total soil mass that can be eroded from and deposited at each cell. The reasoning is that when soil erodes or deposits, changes occur in the elevation at each point of erosion or deposition. The elevation height varies dynamically. However, the soil erosion and deposition function I developed does not account for such changes, i.e., the underlying Digital Elevation Model (DEM) does not change.

If more than a critical amount of soil is deposited within a local area, water may stop flowing in towards it and so less soil will be deposited. Vice versa, if soil erodes within a local area, more water may flow into it and cause more influx of sediment but also potentially greater erosion due to greater overland flow. In this study, the critical limit is set to 10kg per square meter as an example limit. This assures that the function does not produce persistently high unrealistic erosion values for any cells. Therefore, the output Net Erosion/Deposition (presented in the previous section) should not pass beyond +/- 10 and Net Erosion should not pass below -10 for a simulation run based on a resolution of 1m. In a cell where the critical limit for erosion is reached, no more erosion can occur during the simulation. Likewise, no more deposition can occur if the critical limit for deposition has been reached, and suspended sediment will instead continue to be routed with the flow algorithm.

Additionally, a water depth limit is set for where transport of sediment mass can occur to other cells. This limit was included to maintain some realism in how much water is required to transport any sediment mass: for example, a cubic millimetre spread out across a cell would probably not be able to transport any substantial number of particles. In this study, the limit was set to 1.5 mm water depth per square meter.

3.3 Set of equations for erosion and deposition

In this section the variables used for estimating soil erosion and deposition are presented in detail, including the LISEM set of equations for splash erosion, overland flow erosion and transport capacity. Importantly, this study uses a median grain diameter of 50 µm which has been previously used in several studies involving LISEM (Starkloff & Stolte 2014; Jerszurki et al. 2022).

3.3.1 Splash erosion

The equation for splash detachment is dependent on the kinetic energy of the rainfall as it impacts the ground surface. It accounts for that kinetic energy impacting the ground decreases as it dissipates through the layer of runoff water depth increases:

$$Ds = \left(\left(\frac{2.82}{As}\right) * Ke * e^{-1.48*h} + 2.96\right) * \mathrm{P} * \mathrm{A} * \mathrm{dt} \qquad (2)$$

where:
Ds = splash detachment [kg m^{-2} s^{-1}]
As = aggregate stability, median number of drops to decrease aggregate mass by 50% [unitless]
Ke = kinetic energy of rainfall [J m^{-2} mm^{-1}]
h = depth of surface water [mm]
P = precipitation (without plant cover) or precipitation subtracted by interception (with plant cover) [mm]
A = surface area of splash [m^2]
dt = time of time-step [s]
(Jetten 2018).

How kinetic energy is calculated in LISEM depends on whether the rain falls freely on bare soil (Ke_r) or if it is intercepted by and falls through ground covering plants (Ke_t).

$$Ke_r = 8.95 + 8.44 * \log(Ri) \qquad (3)$$

$$Ke_t = 15.8 * \left(h_p\right)^{0.5} - 5.87 \qquad (4)$$

where:
Ri = rainfall intensity [mm/h] (Starkloff & Stolte 2014)
h_p = plant height [m]
(Jetten 2018).

3.3.2 Overland flow erosion

Overland flow detachment is calculated as:

$$Df = Y * (Tc - Sc) * Sv * dt * dx * \delta \qquad (5)$$

where:
Df = overland flow detachment [kg m^{-2} s^{-1}]
Y = erosion efficiency coefficient [unitless]
Tc = transport capacity [kg m^{-3}]
Sc = sediment concentration [kg m^{-3}]
Sv = settling velocity of particle as per Stokes' law [m s^{-1}]
dt = time [s]
dx = length of slope (grid cell length) [m]
(Starkloff & Stolte 2014)
and
δ = flow width/cell width [m]
(Jetten 2018)

The erosion efficiency coefficient is calculated through:

$$Y = 1/(0.89 + 0.56\left(COH_s + COH_p\right)) \qquad (6)$$

where:
COH_s = cohesion of soil [kPa]
COH_p = additional cohesion from plant roots [kPa]
(Jetten 2018).

Transport capacity refers to the maximum concentration of sediment that the flow of surface runoff can transport before deposition occurs (Jetten 2018). The set of equations used to calculate transport capacity are functional only for particles greater than 32 µm (UTwente, n.d. -b). They are:

$$Tc = \chi * \left(S * v_q * 100 - CSP\right) * \varepsilon \qquad (7)$$

where:
Tc = transport capacity [kg m^{-3}]
S = sine of slope [unitless]
v_q = flow velocity [m s^{-1}]
$\chi = ((D50 + 5)/0.32)^{-0.6}$, where D50 is the median grain size [µm]
$\varepsilon = ((D50 + 5)/300)^{0.25}$
CSP = critical stream power [0.4cm s^{-1}]
(Govers 1990)

Settling velocity is calculated as:

$$Sv = R * g * D^2/(C1 * v + (0.75 * C2 * R * g * D^3)^{0.5} \qquad (8)$$

where:
R = submerged specific gravity [1.65 for quartz in water]
g = acceleration due to gravity [m s^{-2}]
C1 = constant 1 [18 for smooth spheres]
C2 = constant 2 [0.4 for smooth spheres]
D = diameter of particle [m]
v = kinematic viscosity of fluid [m^2 s^{-1}] [$1*10^{-6}$ for water]
(Ferguson & Church 2004).

3.3.3 Deposition and deposition rate

In LISEM, deposition occurs in cells where sediment concentration is greater than transport capacity (Sc > Tc), since the runoff flow during such conditions contain a greater sediment concentration than what can transported by the flow (Jetten 2018). This logic is also applied in this study when calculating the weight of deposited sediment mass (kg) in a cell. However, while LISEM uses a deposition rate based on Stokes' law for settling velocity to calculate the deposition weight for all cells in any given time step (Jetten 2018), I will try to use a different approach that assumes that sediment will deposit after a fixed time: If sediment concentration has continuously been greater than transport capacity in a cell for a total of 300 seconds, then:

$$Dp = W_s \qquad (9)$$

where:

Dp = sediment deposition [kg m^{-2} s^{-1}]
W_s = Suspended sediment weight in cell [kg]

This tries to emulate the phenomenon of that sediment deposition in water occurs over time rather than instantaneously, while making the calculation simple.

3.4 Testing the newly implemented soil erosion and deposition function

The soil erosion and deposition function will first be tested on four mathematical surfaces (Fig. 12) and then on a whole watershed (Fig. 13). When the mathematical surfaces are used in water flow simulation, the convex surface results in divergent flow to the edges of the area where the outlet is, while the concave surface results in convergent flow to the centrally located outlet (Zhou & Liu 2002). Meanwhile, the saddle contains a mixture of convex and concave slopes; the resulting flow is diverging across the saddle and converging along the saddle or is near parallel (Zhou & Liu 2002). Lastly, in the plane surface the slope and aspect are unchanged, and the flow is parallel towards the outlet (Zhou & Liu 2002).

As such, the expected logic of the soil erosion and deposition function is that suspended sediment will be transported proportionally with water flow (divergently, convergently, or parallel) to the outlets. Testing the function on these mathematical surfaces will therefore help in understanding if the function predicts erosion and deposition transport in runoff according to the logic of the flow.

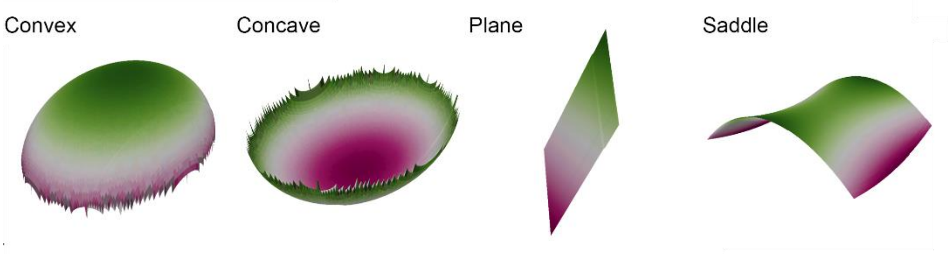

Figure 12. Mathematical surfaces for testing the soil erosion and deposition function.

In difference, testing the soil erosion and deposition function for a whole watershed will enable to see how the model performs in a realistic scenario where all upstream contributing area contributing to the water flow (flow accumulation) is accounted for and where edge effects can be avoided. The watershed area is 789 ha and has undergone field measurements of sediment (Linefur et al. 2021; SLU n.d.). However, the purpose of simulating the model for this area is not to compare the output with field measurements, but rather to check if the distribution of soil erosion, sediment transport and soil deposition happen according to the expected logic.

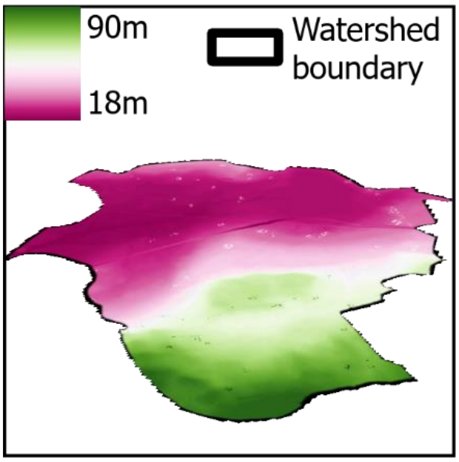

Figure 13. Watershed area M36 in 3D-view. Geodata sources: Land Survey (2019), Swedish Environmental Protection Agency (provided by Stefan Andersson, 2023)

In the coming sections, I will present the input data for the set of LISEM and TFM-DYN for both the mathematical surfaces and the watershed. Values of some input data are shared for both the mathematical surfaces and the watershed while others are unique and more heterogeneous. This is because the watershed simulation attempts a more realistic simulation that requires more heterogeneity in terms of variable values, while for the mathematical surfaces it is helpful to homogenise several variables values to test the underlying logic more easily in without interference from complicating value intervals.

3.4.1 Input data for TFM-DYN

The input for TFM-DYN consists of a temporal dataset that describes rainfall intensity during the simulated rain event, and three spatial datasets of elevation, infiltration capacity and surface friction. Other input data, e.g. the underground storm water network is not valid for the study and hence not used.

Temporal rainfall intensity data for a single rainfall event

To test the soil erosion function's performance a time series is used corresponding to the duration of a 1.5-hour rainfall event that describes rainfall intensity per 15 minutes (Fig. 14). An additional 0.5 hours of run-time of the model is added to see how the soil erosion and deposition function behaves after the rain event has stopped. The rainfall intensity values are made up and inspired by the largest downpour recorded on a measurement station in Stockholm (Stockholms stad 2023).

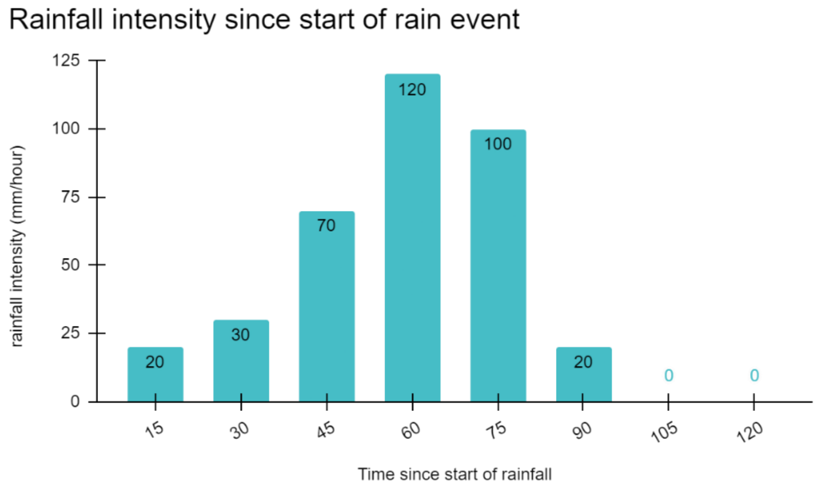

Figure 14. Hyetograph of rainfall event used in TFM-DYN to test the soil erosion and deposition function

Elevation

Elevation is represented by Digital Elevation Models (DEMs) with 5m spatial resolution for the mathematical surfaces and 2m spatial resolution for the watershed.

Infiltration capacity and surface friction

The infiltration capacity will be an input function depending on soil type and duration of rain in TFM-DYN simulation. However, crust formation is not calculated but its effect is implicitly included in the infiltration function. Meanwhile, the surface friction values will affect the portions of water transferred to neighbour cells in each time step (it can slow down velocity) which will also influence how much suspended sediment from splash and overland flow erosion that are transferred (see Fig. 11).

For the mathematical surfaces infiltration capacity and surface friction are set to single uniform values for each cell (no spatial variation), while for the watershed, the infiltration capacity and friction depend on the spatial variation of soil types and land use types respectively. The infiltration capacity of different soils was set within the range 0-210 mm/h (Berhanu et al. 2013) and surface friction to 0.013-0.2 (Van der Sande 2003). More sandy soils were given a higher infiltration velocity.

3.4.2 Input data for LISEM variables

For the mathematical surfaces the LISEM variables are also set to a single uniform value for each cell with no spatial variation (Table 1). For the watershed, the LISEM variables are set based on earlier studies (Starkloff & Stolte 2014; Jerszurki et al. 2022). Some are treated as single integer values, such as median grain size D50 and submerged specific gravity R, while others are treated as intervals and therefore has a spatial distribution. The interval variables depend on the spatial variation of soil types and land use types respectively.

Table 1. LISEM variables and their values used for simulations on mathematical surfaces and watershed respectively

LISEM variables					
Shared values for mathematical surfaces and watershed simulations		Unique values for mathematical surfaces		Multiple unique values for watershed	
Critical Stream Power	0.4	Precip throughfall	0	Precip throughfall	
Constant 1	18	Plant height	1	Plant height	0, 0.4, 0.5, 20
Constant 2	0.4	Additional cohesiveness from roots	1	Additional cohesiveness from roots	1, 3.32, 5, 10, 999
Submerged Specific Gravity	1.65	Soil cohesiveness	1	Soil Cohesiveness	1.35 , 3.32, 20, 999
Gravity Acceleration	9.82	Aggregate stability	1	Aggregate stability	1, 26, 66, 200
Kinematic Viscocity Water	0.000001				
Diameter of soil particle	50				

3.4.3 Expected logical predictions of soil erosion, sediment transport and deposition

The erosion and deposition predictions of the soil erosion and deposition function are expected to follow a certain logic according to theories of soil erosion. For example, during high intensity rainfall, more rainsplash erosion is expected to occur due to the increased energy from the rainfall (Morgan 2005). Furthermore, in areas of high slope the increased flow velocity is expected to erode more particles (Morgan 2005). Vice versa, in areas of very low slope where flow velocity is lower, the lack of transport capacity of the flow should cause deposition (Haan et al. 1994, as cited in Mitasova 2013). Logically therefore, as another example, continuously high slopes are expected to transport particles in the direction of the slope until the slope decreases enough upon which deposition is expected.

The purpose of the four mathematical surfaces (convex, concave, plane and saddle) is to evaluate the performance of the soil erosion and deposition function in relation to this expected logic. This is carried out through visual impressions of the main output variable Net Erosion/Deposition.

Another expected logic is that erosion should only occur where the input variables allow for it in a heterogeneous natural landscape. For example, areas with low soil cohesiveness and no plant cover that offers additional cohesiveness from roots, as well as low aggregate stability, are expected to be greater sources of erosion than areas with opposite characteristics. The watershed simulation is a way of evaluating this logic, although it will be more difficult since the shape of the elevation is much more complex. Additionally, since the input variables for the watershed simulation will have multiple values (Table 1) the expected logic will be harder to evaluate solely based on visual impression of the Net Erosion/Deposition output.

4. Result

This section presents the output of the TFM-DYN model with the added soil erosion and deposition functionality. The main output of the model is Net Erosion/Deposition (NED), which is the balance between accumulation of erosion and deposition in each cell at a given time step of the simulation. The unit is kg. If the value is negative, it signifies greater erosion than deposition in that cell, and vice versa. First the simulation output based on the mathematical surfaces is presented, and then the simulation output based on a watershed.

4.1 Simulation of mathematical surfaces

In this section, the simulation output of the mathematical surfaces (convex, concave, plane, and saddle) is presented. The output is displayed through one 3D-visualisation and one graph for each surface respectively. First, I will describe the 3D-visualisations (Fig. 15a-d), and secondly the graphs (Fig. 16a-d). Finally, Fig. 17 is a more detailed version of Fig. 16b.

Fig. 15a-d shows, for each surface, a time series of NED during four time steps of the rain event. At the first time step, time step 1200 (after 20 minutes), the spatial distribution of NED follows the same trend for all surfaces: net erosion has occurred faintly across most cells, and it is generally greater where slope is greater. At the second time step, time step 2100 (35 minutes), this pattern is now more pronounced for all surfaces. However, there is also a hint of deposition occurring at the centre of the saddle, convex and concave surfaces where there is little to no slope. Meanwhile, there is no indication of deposition in the plane surface. This seems to meet the expected logic, as the plane's whole surface has a constant slope which prevents deposition from occurring, as transport capacity increases enough for only erosion to occur.

At the third time step, time step 5400 (after 90 minutes), the accumulated erosion has increased substantially for all surfaces. This could be due to that the whole period of precipitation has now already happened and overland flow erosion and rainsplash erosion have both piled up. Notably, among the areas covered with high net erosion, there are also a few thin areas of lesser erosion. Meanwhile, the smaller areas of deposition visible in the earlier time step have now become clearer, which indicates that deposition has also increased at these fewer cells. At the last time step, time step 7200 (after 120 minutes), the thin areas visible in the previous time step have smoothed out, and the maximum net deposition has also increased clearly visibly.

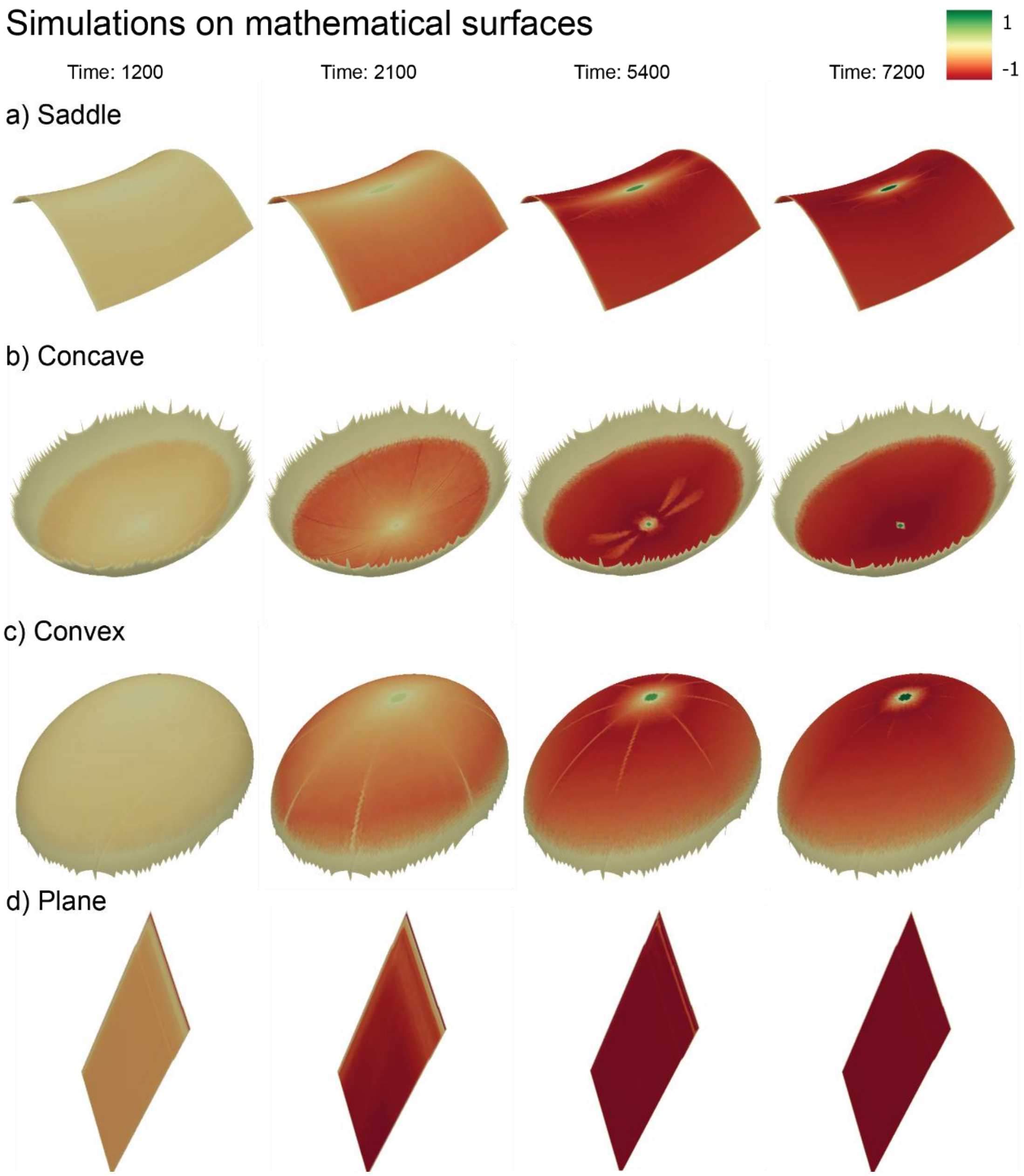

Figure 15a-d. Net Erosion/Deposition (NED) at the end of the rainfall simulation (time step 7200) for each mathematical surface (a-d). NED is an accumulated balance between erosion and deposition in each cell. The values shown are normalised NED to compare the relative intensity of erosion and deposition more easily across the different surfaces. The time unit is in seconds. The simulations show that small amounts of erosion covers most of the surface initially, where slope is greater, and then increases rapidly as the rainfall intensity increases.

Fig. 16a-d show one graph per mathematical surface; each graph plots five output variables for a single cell that are registered at intervals of 300 seconds throughout the rain event. The variables are NED, net erosion, transport capacity and sediment concentration and sediment weight. The plotting of these variables offer a supplementary understanding of the main output of the model (NED). Net erosion is an accumulated measure of erosion in the cell and is the same variable as NED except that it excludes deposition, and, importantly, it treats erosion values as absolute (positive) rather than negative to differentiate them from NED in the graphs. Lastly, the variables transport capacity and sediment concentration are described in Section 3.3, and sediment weight is described in Section 3.3.3.

Firstly, the saddle surface, NED rises over time, meaning that deposition occurs from influx of suspended sediment until around 5000 seconds, or about 83 minutes, into the rain event; 7 minutes before the end of rainfall. The influx of sediment may have stopped towards the end of the rainfall since rainsplash and overland flow erosion decrease. Also, transport capacity is very low likely because there is little to no water flow. Since sediment weight and concentration is stored after deposition, the values of these variables are also close to zero.

Secondly, for the concave surface, net erosion can be seen as the inverse of NED, meaning that no deposition is occurring so that only erosion is influencing the NED value. For most of the rain event, transport capacity is slightly higher or equal to sediment concentration, which means that erosion can occur. The amount of eroded sediment varies over time, until it reaches the limit of 250kg as mentioned in Section 3.2.6. The graph also shows the sediment weight in the cell that is still in the cell at the end of each timestep, meaning it has not had time to be transported to another cell by the TFM-DYN algorithm. The concave surface plot is like that of the plane surface. However, in the plane surface the transport capacity rises quicker and simultaneously erosion as well.

Lastly, for the convex surface, erosion is occurring with a comparatively lesser amount of erosion. Yet the transport capacity is close to 0. The reason is that the model assumes that erosion from rainsplash will occur regardless of transport capacity in the cell.

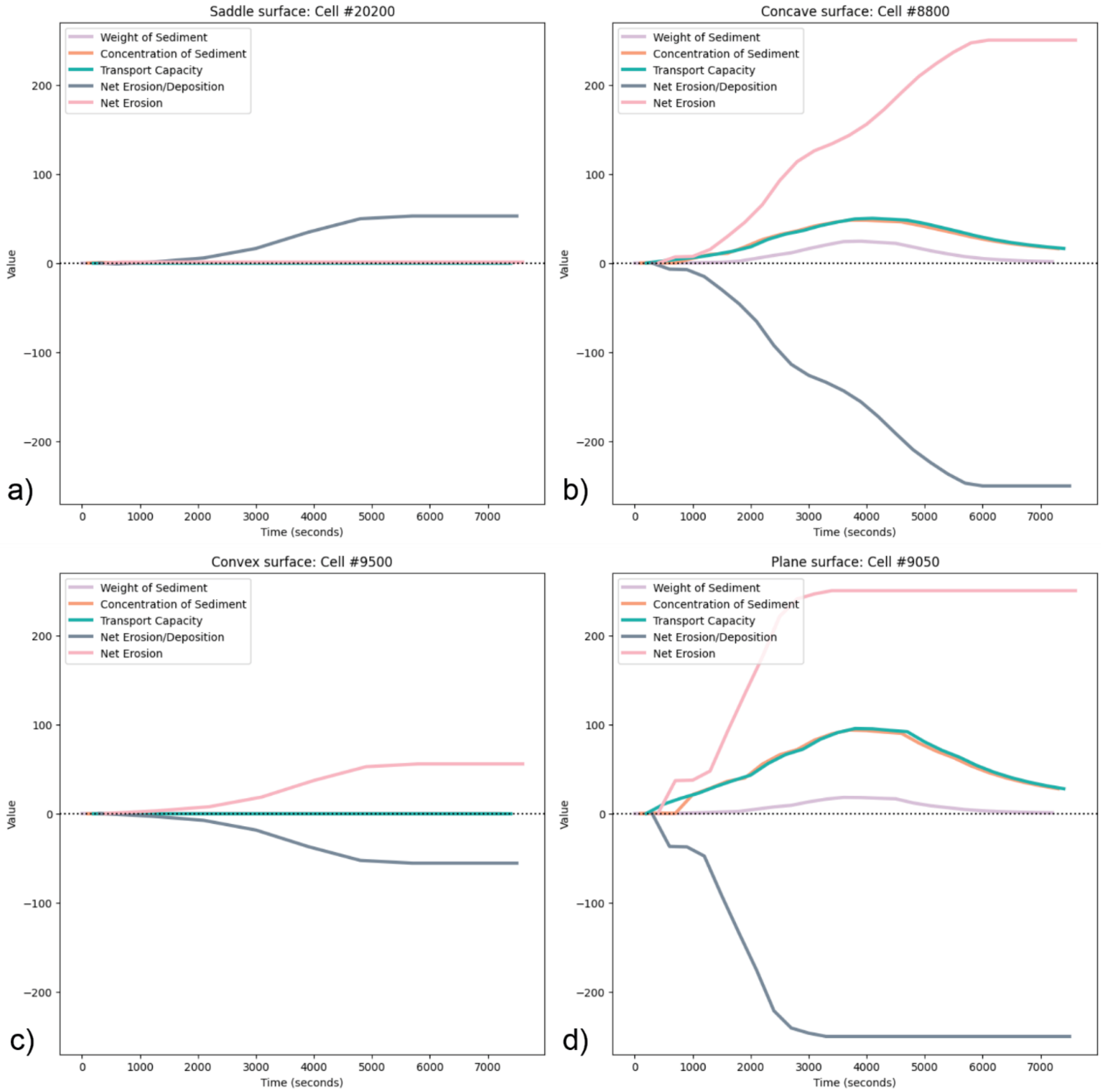

Figure 16a-d. Five variables of soil erosion and deposition function at one cell in each of the four mathematical surfaces (a-d). Negative values of Net Erosion/Deposition represent net erosion, and positive values represent net deposition. A value of 0 means that neither erosion nor deposition has occurred. The variable Net Erosion is the inverse (absolute) value of net erosion in Net Erosion/Deposition, to distinguish these two variables more easily from one another.

To illustrate the relationship between relevant variables in greater detail, Fig. 17 shows the same concave surface cell as in Fig. 16b with two additional variables (the weight of overland flow erosion and splash erosion) and normalised values for easier comparison between all variables. It shows that splash erosion is independent of if Tc > Sc or not, since it is related to rainfall intensity, while overland flow erosion indeed is dependent on that Tc > Sc, as well as the magnitude of the difference between Tc and Sc where Tc > Sc.

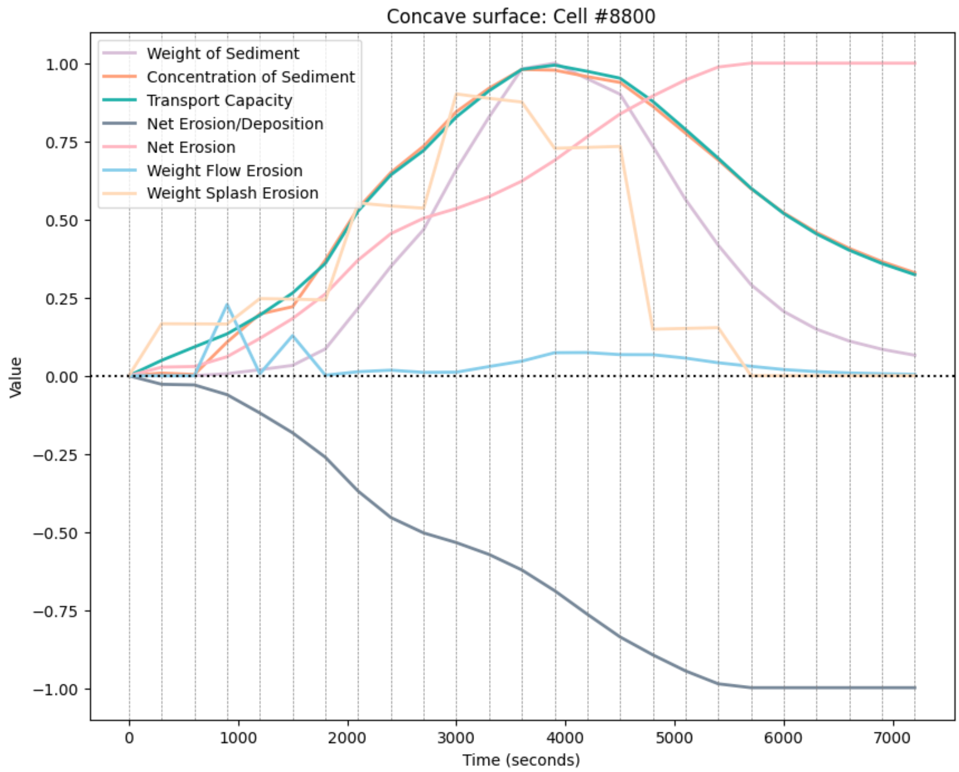

Figure 17. Detailed graph of concave surface cell #8800. This figure is the same as 16b, except that it is more detailed (and with normalised values): it includes two additional variables Weight Flow Erosion (overland flow erosion) and Weight Splash Erosion, as well as tick marks for each recorded time step (vertical gray lines). It shows how splash erosion is rising due to the rise in rainfall intensity. Meanwhile, overland flow erosion is dependent on if Tc > Sc, and the magnitude of the difference between them when Tc > Sc. The wavy appearance of NED (and Net Erosion) can be explained by the addition or absence of overland flow erosion at various time steps.

4.2 Test simulation of soil erosion and deposition on real catchment area

In this section, the simulation output of NED at the end of the rainfall event (time step 7200) of the whole watershed is presented (Fig. 18). In terms of accumulated erosion at the end of the rainfall, its distribution pattern seems to largely resemble stream networks that are created from surface runoff. In comparison, the distribution of accumulated deposition seems less concentrated and more spread out across the landscape. However, some relatively higher quantities of deposition seem to accumulate at the end of these above-mentioned stream networks.

Meanwhile, some areas have neither erosion nor deposition, which could be explained by that the input variables constrain erosion (notably on roads), and simultaneously the transport capacity being higher than sediment concentration so that whatever water that flows across the area does not deposit there. Lastly, it may also be because there is little to no upstream area and therefore little influx of suspended sediment.

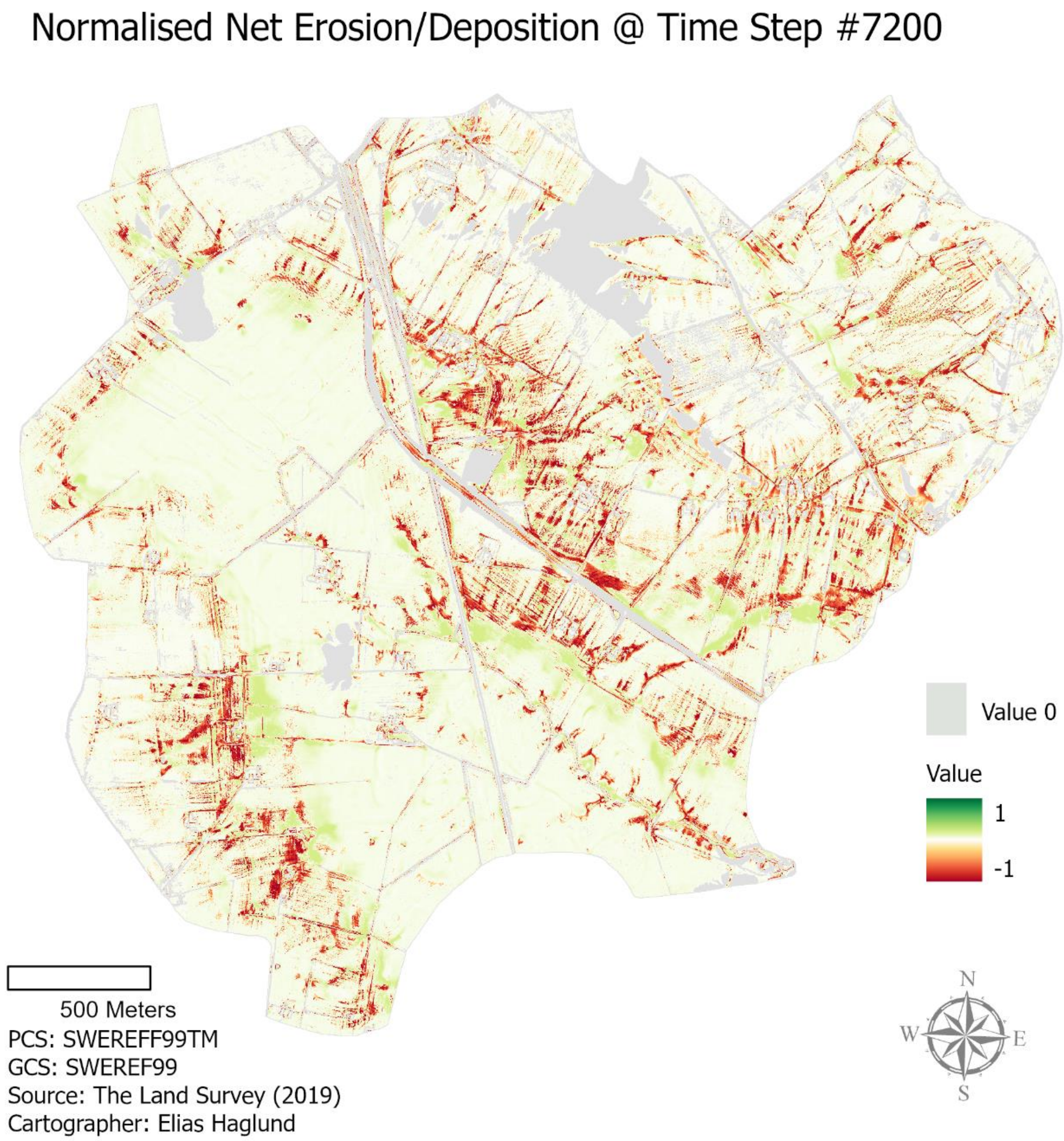

Figure 18. Map showing Net Erosion/Deposition at the end of the watershed simulations. Values are normalised. Value 0 represents no occurrence of accumulated erosion or deposition in cell. Watershed geodata source: Swedish Environmental Protection Agency (provided by Stefan Andersson, 2023)

Notably, the watershed simulation does not use the deposition rate as described in Section 3.3.3. While it worked to produce an expected logic on the mathematical surfaces, upon testing, it turned out to not be feasible in a real planetary landscape. The reason is that sediment concentration rarely is higher than transport capacity for multiple seconds in a row.

Instead, multiple ways of calculating deposition were tested for the watershed: I multiplied the suspended sediment weight in each cell with a) the fraction of sediment concentration that corresponds to the suspended sediment weight that is greater than what the water flow can transport (transport capacity) and b) the estimated settling time of a particle per time step. I tried several ways of estimating the settling time of a particle, namely 1) simply using a fixed time, such as 300 seconds or 2) to divide the water depth with a particle's settling velocity according to Stokes' law (Starkloff & Stolte 2014). By assuming that the deposition rate would increase during the rain event, I also tried to replace b) with 1 divided by the division of total simulation time (7200 seconds) subtracted by current time step (for example time step 5000) and the current time step length. Lastly, I also tried the same approach used in LISEM to calculate deposition rate by multiplying settling velocity, flow width and the difference in sediment concentration and transport capacity (Jetten 2018). The map in Fig. 13 is the output of the simulation where deposition was calculated using the above-mentioned approach for calculating settling time of a particle was estimated by dividing water depth with a particle's settling velocity according to Stokes' law.

5. Discussion

In this section, I will discuss some key points of the results of the soil erosion and deposition function regarding the goals, aim and finally the purpose of this study.

5.1 Capabilities of the model

In this study, a mathematical function was implemented in a dynamic triangular flow algorithm as a prototype for soil erosion and deposition prediction. In this section, I will discuss the primary goal of the function, to predict soil erosion, and the two secondary goals of predicting sediment transport and deposition. Simultaneously, I will also address one of the aims of the study, namely, to evaluate whether the function's logic is solid.

Firstly, the results of the simulation of the mathematical surfaces and watershed show that the resulting function is a successful prototype that can dynamically estimate erosion. The output is a numerical weight in kilograms and is a measure of how much soil mass is eroded at each cell location and time step. The erosion accounted for is based both on estimations from rainsplash and overland flow. The set of equations for overland flow erosion specifically address rill erosion (excluding for example gully erosion), just like the LISEM model (Jetten 2018).

The erosion is generally considered to follow the expected logic as outlined in Section 3.4.3. For example, most evident in the mathematical surfaces (Fig. 15a-d), the generation of overland flow erosion is greater at greater slope and water velocities, which follows the expected logic. As for the watershed simulation (Fig. 18), the output mass of erosion is also largely dependent on the input variables of the set of LISEM equations and of the TFM-DYN model that together describe the resistance and protection characteristics of a land cover (Morgan 2005; Jetten 2018; Nilsson et al. 2022). This makes it harder to pinpoint the reason to why certain areas display accumulated erosion. However, there are also examples to be found in this simulation of how erosion follows the expected logic. For example, the watershed showed zero erosion at certain areas such as asphalt roads where aggregate stability and soil cohesiveness were set to high values. Vice versa, the largest clusters of erosion seem to have formed along stream networks modelled by the MFD flow algorithm of the TFM-DYN model. This is also an expected logic, as transport capacity, a main driver of overland flow erosion in the function, is larger in stream networks where flow velocity is generally greater.

Notably, the eroded weight was limited to 10kg per square meter in the model, since I assumed there would be a finite amount of soil that could be eroded during a given rainfall. As such, the level of erosion peaked at 40kg per cell for the watershed surface of resolution 2 m^2. This limit also accounts for cells that may produce persistently high unrealistic erosion values. This phenomenon can occur while working with several diverse input variables, or also due to bugs that may have appeared while coding for the implementation of the function into the dynamic flow algorithm. In the case of the watershed, only a tiny minority of cells with negative NED values (where net erosion occurred) reached this limit, which means that most cells did not produce unrealistically high values. However, being a prototype, input variables should be calibrated (Bennett et al. 2013) and potential bugs should be tested for.

To summarise, the primary goal of successfully modelling soil erosion within the TFM-DYN model can be considered to have been achieved. That is, the function behaves according to the expected logic. That said, there is room for calibration and debugging.

The secondary goals of modelling the transportation and subsequent deposition of suspended sediment (once eroded) were helped by the TFM-DYN's MFD flow algorithm. This is visible in the mathematical surfaces where deposition almost exclusively occurred where the slope is so low that the velocities in those cells, as calculated by TFM DYN, became too low for transport capacity to build up (Fig graph). As such, concentration capacity was higher for more than 300 seconds worth of time steps deposition occurred. This is therefore an expected logic. Furthermore, the transport and deposition downstream also appear visible in the watershed simulation, where the deposition of sediment seems to mainly occur downstream from stream networks. The visual impression is therefore that the model can logically predict where eroded sediment should deposit.

In terms of simulating sediment transport, the dynamic triangular algorithm TFM-DYN used as a "host" for the soil erosion and deposition function inspired by LISEM enables a prediction of the spatial distribution of soil mass. If the functionality had been added to a static model, such as the D8, the output would fail to reflect how sediment is transported with water in multiple directions from a given cell; erosion and deposition would not occur across the landscape, but in a narrow one cell-wide channel (Epple et al. 2022). Also, the lack of velocity in a static model also would unable the current use of the LISEM equation for overland flow erosion.

The fact that the implemented function can also account for re-suspension (re-erosion) and re-deposition of already eroded and deposited sediment, means that it can predict how soil mass may be erratically transported across space during real rain events. The resulting mass of eroded and deposited soil reflects the characteristics of the land (such as soil type, land use and friction) and the attributes of the rain event (such as rainfall intensity, spatial distribution of rain and interception).

In terms of simulating sediment deposition, similarly to for erosion, deposition was set to a limit of 10kg on the assumption that it is unrealistic for many areas in a real landscape to receive a higher amount of deposition. The reason is that once deposition reaches a certain weight in an area, the area will get an increased elevation, which in turn could influence the routing of sediment. However, instead of using fixed limits of deposition, this phenomenon could be addressed differently by allowing for the DEM itself to change by deposition. That would allow for rerouting of sediment to nearby cells, while also not needing a fixed limit to deposition. It would add a relevant dynamic perspective of how elevation changes over time through soil erosion.

Furthermore, transport capacity is an important variable in determining whether erosion or deposition occurs at each time step and cell. The principle is that deposition occurs, just like in the original LISEM model (Jetten 2018), where $Sc > Tc$; the "surplus" sediment concentration greater than transport capacity is deposited at a particular rate. This is illustrated in Fig. 16a-d and in detail in Fig. 17. As such, using transport capacity seems to work equally well in this study's soil erosion and deposition function as in LISEM in this regard.

However, the method for estimating deposition rate used in LISEM, which is based on the variable settling velocity (Jetten 2018), did not work as intended in the developed function. More experimentation could be carried out to understand why that is. Instead, the method that best met the expected logic for the simulations on mathematical surfaces is the one outlined in Section 3.3.3. For this method, the time length 300 seconds was chosen since it produced a significant amount of deposition. By significant, I mean that the amount of deposition should be in the same order of magnitude as erosion, but smaller, since a lot of eroded particles could still be suspended in water flow or could have left the flow outlet of the surface entirely and thus would not deposit. For example, when time was increased to 500 seconds during experimentation, much less deposition would occur (even though the spatial distribution of deposition was be similar to that of using time 300 seconds). This make sense, since it would take a longer time for deposition to be able to occur. To determine an optimal time length, calibration could be used (Wainwright & Mulligan 2012).

However, a weakness in this method is that the deposited sediment weight is based on the suspended sediment that is in the cell after 300 seconds, rather than continuously depositing surplus sediment concentration where $Sc > Tc$. The previously mentioned principle for deposition is therefore not followed in a realistic manner; the function should deposit the amount of sediment at a fixed deposition rate (settling velocity) at each time step, rather than depositing all sediment after 300 seconds. However, even though the deposition rate is not behaving entirely realistically, it still fulfills the expected logic of how deposition ought to behave on mathematical surfaces.

To summarise, sediment transport and deposition are occurring in a distributed fashion according to the expected logic. However, the study is inconclusive in which manner the deposition rate should be calculated. Ideally, the deposition rate method should both be realistic in theory and meet the expected logic in the simulation output. Also, as it is now, I used different methods for calculating deposition rate for the mathematical surfaces and the watershed respectively. Ideally, as well, there should be only one method to estimate deposition rate for both types of surfaces. For this reason, more investigation is needed.

5.2 Combining two models

The second aim of this study was to understand how a soil erosion functionality can be implemented in a dynamic triangular algorithm. In this study, the choice was to use a set of equations from an already existing distributed soil erosion and deposition model (LISEM). Compared to lumped empirical models such as USLE which are only applicable for larger temporal periods and spatial areas such as watersheds (Renard et al. 2017), LISEM offers a set of equations that already work on a cell-by-cell basis where the resolution is flexible (Jetten 2018). As such, little adaptation was needed to implement the equations into the TFM-DYN model.

That said, while implementing a set of equations into a model like TFM-DYN, there was a level of interpretation needed for how the equations should be integrated into the model. This included not only adjusting the equations to the existing model structure of TFM-DYN, but also to how it was constructed by the programming language Python, as well as the capabilities and limitations of this language itself. Making sure the code is both able to run efficiently and stay true to the expected logic and equations that are used is a continuous challenge with every iteration of the soil erosion and deposition function.

5.3 Addition to the fields of environmental modelling and landscape architecture, planning and management

The purpose of this study has been to contribute to the on-going development of effective and useful soil erosion and deposition prediction models within the fields of environmental modelling research, and landscape architecture, planning and management respectively.

Given today that, to my knowledge, no such studies exist of a dynamic triangular flow algorithm with a soil erosion and deposition functionality, this study has contributed with a unique prototype of a soil erosion model to environmental modelling research. Furthermore, the model is applicable within landscape architecture, planning and management as shown in this study: The model works on a watershed scale, but on a greater local scale, since TFM-DYN allows for high resolution simulations (Nilsson et al. 2022). Higher resolution simulations could allow for more heterogeneous input data to be used, and the predicted rainsplash and overland flow erosion would scale accordingly. This could be beneficial for example in detailed studies within spatial risk assessment (Guo et al. 2021), and several applications of landscape ecology or urban planning (Turner & Gardner 2015; Qian et al. 2015). To iterate Section 1.1, for soil erosion models to be effective tools in spatial risk assessment on a detailed landscape scale, and thus be relevant for local management, they need to reflect spatial hetereogeneity of erosion on that scale (Berberoglu et al. 2020). This is what a soil erosion and deposition functionality can achieve once implemented in TFM-DYN.

However, for a smaller study area than a watershed, one may need to account for the influence of soil erosion and deposition from upstream areas. This would be particularly relevant to consider if one would have a dynamic DEM that changed with fluxes of deposition, as discussed in Section 5.1, as increasing amount of upstream area could lead to increased deposition in the study area.

5.4 Conclusion

In this conclusion, I will respond to the research questions posed in the introduction of this study.

1. What are the benefits of using a dynamic triangular flow algorithm to model soil erosion, sediment transport through water, and soil deposition?

    a. It can act as a “host” for a functionality of soil erosion and sediment transport and deposition.

    b. The input variables of soil erosion and deposition may be calculated through certain output variables of the algorithm, such as flow velocity.

    c. Within the field of landscape architecture, planning and management, it can benefit by modelling high-resolution patterns of distribution of soil erosion and deposition in planetary landscapes. This could be helpful in spatial risk assessment of erosion, and to help land managers determine where in a natural landscape preventionary measures such as increasing plant cover and introduction of ecological succession could mitigate erosion most effectively.

2. How can a mathematical function be added into a dynamic triangular flow algorithm to create a prototype soil erosion and deposition prediction functionality?

    a. This study showed that using a set of equations based on an already existing soil erosion model that works on a cell-by-cell basis was a feasible approach.

    b. However, some interpretation and adjustment of variables may be needed over several iterations of prototyping. As such, having a good experiment structure for repeated testing is valuable.

3. How can the logic of the resulting prototype soil erosion and deposition function be evaluated?

    a. A simple way to visually assess the logic of the prototype is to use mathematical surfaces that test whether the erosion (rainsplash and overland flow), sediment transport and deposition occurs according to the expected logic. Additionally, by also running a simulation on a watershed in a natural landscape, the model can be tested for real circumstances.

    b. Although it was outside the scope of this study, using methods of validation and calibration are additional methods which are necessary to determine the accuracy of the model.

5.5 Method reflection

In this study, the method for adding the soil erosion and deposition function into TFM-DYN involved a few different aspects. In this section I will reflect on some of these aspects, both in terms of what worked and what could have been done differently.

Firstly, a literature review was carried out partly to understand the fundamentals of soil erosion and deposition, and partly to get insights about environmental modelling in general, and specifically what types of soil erosion and deposition models and hydrological models that have been used widely up until today, and how they can be categorised. Altogether, the literature review was helpful in narrowing down what type of soil erosion and deposition model that could be appropriate for the integration into TFM-DYN. The choice fell on LISEM as it had the possibility of predicting both rainfall erosion, overland erosion, and deposition on a raster cell in kilogram per second basis. The choice of TFM-DYN as a host for the set of LISEM equations was made since it is an intermediate-complexity dynamic triangular flow algorithm whose source code I received access to for the academic purpose of this study. However, in hindsight, it would have been helpful to carry out a more comprehensive research of existing soil erosion and deposition models that compute erosion and deposition on a raster cell basis in weight per second or similar. Due to the sheer number of models that has been created to estimate soil erosion and deposition, several models might have been relevant to prototype with. This would then have enabled a comparison of the performance of different models.

Secondly, in an environmental modelling approach, I prototyped the soil erosion and deposition function inspired by LISEM into TFM-DYN. This was an iterative process that involved creating multiple versions of the model with the added functionality and presenting them to my supervisor to receive feedback for further iterations. The work was carried out using the programming language Python and the software PyCharm, which were quite helpful since they offered me a lot of control and possibility to tinker with various functions in the source code to accommodate the implementation of the set of LISEM equations. Altogether, the iteration process and the testing using Python were key in completing the study.

Lastly, while a quantifiable way of evaluating the accuracy of the soil erosion and deposition function developed in this study was outside the scope of this study, it is worth to stress the importance of evaluating the accuracy of soil erosion models (Batista et al. 2019). As described in the literature review, which itself is (figuratively speaking) only scraping the surface of soil erosion theory, there is a lot of complexity regarding the phenomena of soil erosion and deposition to consider. A rigorous validation process would be desirable to evaluate the performance and, for example the goodness-of-fit, of the output function (see e.g., Bakker et al. 2005).

5.6 Future studies

Regarding the implementation of a prototype soil erosion and deposition functionality in a dynamic triangular flow algorithm, there are several aspects to explore further. Firstly, future studies could deepen the realism of the function design in several ways. For this study, the output mass of erosion is valid for a theoretical median soil particle size of a diameter of 50µm, however, future iterations could include multiple particle sizes, such as silt, sand, small and large aggregates, or SOM (Foster 2013). This would allow an understanding of how different land covers with different soil particle fractions contribute differently to erosion, sediment transport and deposition. One could also consider adding a spatially distributed limit to how much soil there is to be eroded depending on for example soil type (Foster 2013). Lastly, other forms of erosion, such as stream or gully erosion, could be considered (Fig. 2; Jetten 2018).

Secondly, future studies could also explore the usage of other equations for erosion and deposition other than ones present in the LISEM model. This could be a way to solve the current problem of how to determine deposition rate. There is a plethora of different models and their equations to be inspired by (Borrelli 2021).

References

Scientific literature

Aiello, A., Adamo, M. & Canora, F. (2015). Remote sensing and GIS to assess soil erosion with RUSLE3D and USPED at river basin scale in southern Italy. *CATENA*, 131, 174–185. https://doi.org/10.1016/j.catena.2015.04.003

Alewell, C., Borrelli, P., Meusburger, K., & Panagos, P. (2019). Using the USLE: Chances, challenges and limitations of soil erosion modelling. *International Soil and Water Conservation Research*, 7(3), 203–225. https://doi.org/10.1016/j.iswcr.2019.05.004

Archfield, S.A., Clark, M., Arheimer, B., Hay, L.E., McMillan, H., Kiang, J.E., Seibert, J., Hakala, K., Bock, A., Wagener, T., Farmer, W.H., Andréassian, V., Attinger, S., Viglione, A., Knight, R., Markstrom, S. & Over, T. (2015). Accelerating advances in continental domain hydrologic modeling. *Water Resources Research*, 51 (12), 10078–10091. https://doi.org/10.1002/2015WR017498

Aubry, T.D., Brian F. (1986). Evaluation of Horton's theory of sheetwash and rill erosion on the basis of field experiments. In: *Hillslope Processes*. Routledge.

Bakker, M.M., Govers, G., Kosmas, C., Vanacker, V., Oost, K.V. & Rounsevell, M. (2005). Soil erosion as a driver of land-use change. *Agriculture, Ecosystems & Environment*, 105 (3), 467–481. https://doi.org/10.1016/j.agee.2004.07.009

Batista, P.V.G., Davies, J., Silva, M.L.N. & Quinton, J.N. (2019). On the evaluation of soil erosion models: Are we doing enough? *Earth-Science Reviews*, 197, 102898. https://doi.org/10.1016/j.earscirev.2019.102898

Bennett, N.D., Croke, B.F.W., Guariso, G., Guillaume, J.H.A., Hamilton, S.H., Jakeman, A.J., Marsili-Libelli, S., Newham, L.T.H., Norton, J.P., Perrin, C., Pierce, S.A., Robson, B., Seppelt, R., Voinov, A.A., Fath, B.D. & Andreassian, V. (2013). Characterising performance of environmental models. *Environmental Modelling & Software*, 40, 1–20. https://doi.org/10.1016/j.envsoft.2012.09.011

Berberoglu, S., Cilek, A., Kirkby, M., Irvine, B., & Donmez, C. (2020). Spatial and temporal evaluation of soil erosion in Turkey under climate change scenarios using the Pan-European Soil Erosion Risk Assessment (PESERA) model. *Environmental Monitoring and Assessment*, 192(8), 491. https://doi.org/10.1007/s10661-020-08429-5

Berhanu, B., Melesse, A.M. & Seleshi, Y. (2013). GIS-based hydrological zones and soil geo-database of Ethiopia. *CATENA*, 104, 21–31. https://doi.org/10.1016/j.catena.2012.12.007

Berhe, A.A., Barnes, R.T., Six, J. & Marín-Spiotta, E. (2018). Role of Soil Erosion in Biogeochemical Cycling of Essential Elements: Carbon, Nitrogen, and Phosphorus. *Annual Review of Earth and Planetary Sciences*, 46 (1), 521–548. https://doi.org/10.1146/annurev-earth-082517-010018

Beven (2001). *HESS - How far can we go in distributed hydrological modelling?* https://hess.copernicus.org/articles/5/1/2001/ [2023-07-30]

Bobba, A.G., Singh, V.P. & Bengtsson, L. (2000). Application of environmental models to different hydrological systems. *Ecological Modelling*, 125 (1), 15–49. https://doi.org/10.1016/S0304-3800(99)00175-1

Boiffin, J. & Monnier, G. (1985). Infiltration rate as affected by soil surface crusting caused by rainfall., 1985. Flanders Research Centre for Soil Erosion and Soil Conservation

Boix-Fayos, C., Calvo-Cases, A., Imeson, A.C. & Soriano-Soto, M.D. (2001). Influence of soil properties on the aggregation of some Mediterranean soils and the use of aggregate size and stability as land degradation indicators. *CATENA*, 44 (1), 47–67. https://doi.org/10.1016/S0341-8162(00)00176-4

Borrelli, P., Alewell, C., Alvarez, P., Anache, J.A.A., Baartman, J., Ballabio, C., Bezak, N., Biddoccu, M., Cerdà, A., Chalise, D., Chen, S., Chen, W., De Girolamo, A.M., Gessesse, G.D., Deumlich, D., Diodato, N., Efthimiou, N., Erpul, G., Fiener, P., Freppaz, M., Gentile, F., Gericke, A., Haregeweyn, N., Hu, B., Jeanneau, A., Kaffas, K., Kiani-Harchegani, M., Villuendas, I.L., Li, C., Lombardo, L., López-Vicente, M., Lucas-Borja, M.E., Märker, M., Matthews, F., Miao, C., Mikoš, M., Modugno, S., Möller, M., Naipal, V., Nearing, M., Owusu, S., Panday, D., Patault, E., Patriche, C.V., Poggio, L., Portes, R., Quijano, L., Rahdari, M.R., Renima, M., Ricci, G.F., Rodrigo-Comino, J., Saia, S., Samani, A.N., Schillaci, C., Syrris, V., Kim, H.S., Spinola, D.N., Oliveira, P.T., Teng, H., Thapa, R., Vantas, K., Vieira, D., Yang, J.E., Yin, S., Zema, D.A., Zhao, G. & Panagos, P. (2021). Soil erosion modelling: A global review and statistical analysis. *Science of The Total Environment*, 780, 146494. https://doi.org/10.1016/j.scitotenv.2021.146494

Borrelli, P., Robinson, D.A., Fleischer, L.R., Lugato, E., Ballabio, C., Alewell, C., Meusburger, K., Modugno, S., Schütt, B., Ferro, V., Bagarello, V., Oost, K.V., Montanarella, L. & Panagos, P. (2017). An assessment of the global impact of 21st century land use change on soil erosion. *Nature Communications*, 8 (1), 2013. https://doi.org/10.1038/s41467-017-02142-7

Caon, L., & Vargas, R. (2017). Threats to soils: global trends and perspectives. Global Soil Partnership Food and Agriculture Organization of the United Nations, Brajendra (Eds.) A contribution from the intergovernmental technical panel on soils. Global land outlook working paper.

Chapin, F.S., Matson, P.A. & Vitousek, P.M. (2011). *Principles of Terrestrial Ecosystem Ecology*. Springer New York. https://doi.org/10.1007/978-1-4419-9504-9

Clark, M.P., Bierkens, M.F.P., Samaniego, L., Woods, R.A., Uijlenhoet, R., Bennett, K.E., Pauwels, V.R.N., Cai, X., Wood, A.W. & Peters-Lidard, C.D. (2017). The evolution of process-based hydrologic models: historical challenges and the collective quest for physical realism. *Hydrology and Earth System Sciences*, 21 (7), 3427–3440. https://doi.org/10.5194/hess-21-3427-2017

Clark, T., Foster, L., Bryman, A., & Sloan, L. (2021). Bryman's social research methods. Oxford university press.

De Ploey, J. (1989). A model for headcut retreat in rills and gullies. *CATENA*, 14, 81–86

Desmet, P.J.J. & Govers, G. (1996). A GIS procedure for automatically calculating the USLE LS factor on topographically complex landscape units. *Journal of Soil and Water Conservation*, 51 (5), 427–433

Dotterweich, M. (2013). The history of human-induced soil erosion: Geomorphic legacies, early descriptions and research, and the development of soil conservation—A global synopsis. *Geomorphology*, 201, 1–34. https://doi.org/10.1016/j.geomorph.2013.07.021

Dunne, T. & Aubry, B. (1986). Hillslope Processes. Allen & Unwin.

Earle, S. & Panchuk, K. (2019). Physical Geology - 2nd Edition.

Ekwue et al. (1993). Maximum Bulk Density Achieved During Soil Compaction as Affected by the Incorporation of Three Organic Materials. https://doi.org/10.13031/2013.28515 [2023-07-30]

Epple, L., Kaiser, A., Schindewolf, M., Bienert, A., Lenz, J. & Eltner, A. (2022). A Review on the Possibilities and Challenges of Today's Soil and Soil Surface Assessment Techniques in the Context of Process-Based Soil Erosion Models. *Remote Sensing*, 14 (10), 2468. https://doi.org/10.3390/rs14102468

Evans, R. (1980). Mechanics of water erosion and their spatial and temporal controls: an empirical viewpoint. In, Kirkby, M.J. and Morgan, R.P.C. (eds.). Soil Erosion, Wiley, Chichester. pp. 109–128.

Fatichi, S., Vivoni, E.R., Ogden, F.L., Ivanov, V.Y., Mirus, B., Gochis, D., Downer, C.W., Camporese, M., Davison, J.H., Ebel, B., Jones, N., Kim, J., Mascaro, G., Niswonger, R., Restrepo, P., Rigon, R., Shen, C., Sulis, M. & Tarboton, D. (2016). An overview of current applications, challenges, and future trends in distributed process-based models in hydrology. *Journal of Hydrology*, 537, 45–60. https://doi.org/10.1016/j.jhydrol.2016.03.026

Ferguson, R.I. & Church, M. (2004). A Simple Universal Equation for Grain Settling Velocity. *Journal of Sedimentary Research*, 74 (6), 933–937. https://doi.org/10.1306/051204740933

Fistikoglu, O. & Harmancioglu, N.B. (2002). Integration of GIS with USLE in Assessment of Soil Erosion. *Water Resources Management*, 16 (6), 447–467. https://doi.org/10.1023/A:1022282125760

Foster, G.R. (2013). RUSLE2 Science Documentation.

Foster, G.R., Toy, T.E. & Renard, K.G. (2003). Comparison of the USLE, RUSLE1.06c, and RUSLE2 for Application to Highly Disturbed Lands.

Ghadiri, H. & Payne, D. (1979). Raindrop impact and soil splash. *Soil physical properties and crop production in the tropics*, 95–104

Glasstetter, M. & Prasuhn, V. (1992). Influence on Structural Stability Aggregate Stability. *Erosion, Conservation, and Small-scale Farming*, 285

Govers, G. (1985). Selectivity and transport capacity of thin flows in relation to rill erosion. *CATENA*, 12 (1), 35–49. https://doi.org/10.1016/S0341-8162(85)80003-5

Govers, G. (1990). Empirical relationships for the transport capacity of overland flow.

Govers, G. & Poesen, J. (1988). Assessment of the interrill and rill contributions to total soil loss from an upland field plot. *Geomorphology*, 1 (4), 343–354. https://doi.org/10.1016/0169-555X(88)90006-2

Govers & Poesen (1986). Govers,G.and Poesen,J., F. Callebaut, D. Gabriels, M. de Boodteditors, 19861909437, English, Conference paper, Belgium, Ghent, Assessment of soil surface sealing and crusting, (171–182), Flanders Research Centre for Soil Erosion and Soil Conservation, A field-scale study of surface sealing and compaction on loam and sandy loams soils. Part I. Spatial variability of soil surface sealing and crusting.

Guo, L., Liu, R., Men, C., Wang, Q., Miao, Y., Shoaib, M., Wang, Y., Jiao, L., & Zhang, Y. (2021). Multiscale spatiotemporal characteristics of landscape patterns, hotspots, and influencing factors for soil erosion. *Science of The Total Environment*, 779, 146474. https://doi.org/10.1016/j.scitotenv.2021.146474

Haan, C.T., Barfield, B.J. & Hayes, J.C. (1994). *Design Hydrology and Sedimentology for Small Catchments*. Elsevier.

He, J., Sun, L., Gong, H., Cai, Q. & Jia, L. (2016). The characteristics of rill development and their effects on runoff and sediment yield under different slope gradients. *JOURNAL OF MOUNTAIN SCIENCE*, 13 (3), 397–404. https://doi.org/10.1007/s11629-015-3490-1

Heede, B.H. (1975). Watershed Indicators of Landform Development. https://repository.arizona.edu/handle/10150/300496 [2023-07-13]

Herweg, K. (1996). Field manual for assessment of current erosion damage. University of Berne.

Hjulström, F. (1935). Studies of the morphological activity of rivers as illustrated by the River Fyris. https://www.diva-portal.org/smash/record.jsf?pid=diva2%3A1687693&dswid=-9496 [2023-07-30]

Jerszurki, L., Schultz, G., Jerszurki, D. & Santos, I. (2022). Sensitivity analysis of the OpenLISEM model: calibration for an unpaved road in Southern Brazil. *Modeling Earth Systems and Environment*, 8, 1–14. https://doi.org/10.1007/s40808-021-01288-0

Jetten, V., Govers, G. & Hessel, R. (2003). Erosion models: quality of spatial predictions. *Hydrological Processes*, 17 (5), 887–900. https://doi.org/10.1002/hyp.1168

Kinnell, P.I.A. (2017). A comparison of the abilities of the USLE-M, RUSLE2 and WEPP to model event erosion from bare fallow areas. *Science of The Total Environment*, 596–597, 32–42. https://doi.org/10.1016/j.scitotenv.2017.04.046

Lal, R. (2021). *Soil Organic Matter and Feeding the Future: Environmental and Agronomic Impacts*. 1. ed CRC Press. https://doi.org/10.1201/9781003102762

Linefur, H., Norberg, L., Kyllmar, K., & Blomberg, M. (2021). Växtnäringsförluster i små jordbruksdominerade avrinningsområden 2020/202.

Le Bissonnais, Y. (1990). Experimental study and modelling of soil surface crusting processes. https://www.cabdirect.org/cabdirect/abstract/19911953006 [2023-07-30]

Lenhart, T., Van Rompaey, A., Steegen, A., Fohrer, N., Frede, H.-G. & Govers, G. (2005). Considering spatial distribution and deposition of sediment in lumped and semi-distributed models. *Hydrological Processes*, 19 (3), 785–794. https://doi.org/10.1002/hyp.5616

Lindström, G., Pers, C., Rosberg, J., Strömqvist, J. & Arheimer, B. (2010). Development and testing of the HYPE (Hydrological Predictions for the Environment) water quality model for different spatial scales. *Hydrology Research*, 41 (3–4), 295–319. https://doi.org/10.2166/nh.2010.007

Marsh, H. W., & Hau, K. T. (1996). Assessing goodness of fit: Is parsimony always desirable?. *The journal of experimental education*, *64*(4), 364-390.

Merritt, E. (1984). The identification of four stages during micro-rill development. *Earth Surface Processes and Landforms*, 9 (5), 493–496. https://doi.org/10.1002/esp.3290090510

Miedema, S.A. (2013). Constructing the Shields Curve: Part C — Cohesion by Silt, Hjulstrom, Sundborg. *Proceedings of ASME 2013 32nd International Conference on Ocean, Offshore and Arctic Engineering*, Nantes, France, June 9 2013. V006T10A023. American Society of Mechanical Engineers. https://doi.org/10.1115/OMAE2013-10524

Mitasova, H., Barton, M., Ullah, I., Hofierka, J. & Harmon, R.S. (2013). 3.9 GIS-Based Soil Erosion Modeling. In: Shroder, J.F. (ed.) *Treatise on Geomorphology*. Academic Press. 228–258. https://doi.org/10.1016/B978-0-12-374739-6.00052-X

Montgomery, D.R. (2007). Soil erosion and agricultural sustainability. *Proceedings of the National Academy of Sciences*, 104 (33), 13268–13272. https://doi.org/10.1073/pnas.0611508104

Morgan, R.P.C. (2005). *Soil erosion and conservation*. 3rd ed. Blackwell Pub.

Mutchler, C.K. & Young, R.A. (1975). Soil detachment by raindrops. *ARS-S.*, 40, 113

Nearing, M. A. (2013). Soil erosion and conservation. In J. Wainwright & M. Mulligan (Eds.), Environmental modelling: Finding simplicity in complexity (2nd ed., pp. xxx-xxx). Wiley.

Nilsson, H., Pilesjö, P., Hasan, A. & Persson, A. (2022). Dynamic spatio-temporal flow modeling with raster DEMs. *Transactions in GIS*, 26 (3), 1572–1588. https://doi.org/10.1111/tgis.12870

Okiria, E., Okazawa, H., Noda, K., Kobayashi, Y., Suzuki, S. & Yamazaki, Y. (2022). A Comparative Evaluation of Lumped and Semi-Distributed Conceptual Hydrological Models: Does Model Complexity Enhance Hydrograph Prediction? *Hydrology*, 9 (5), 89. https://doi.org/10.3390/hydrology9050089

Oldeman, L. (1994). An international methodology for an assessment of soil degradation, land georeferenced soils and terrain database. *RAPA Publication (FAO)*,

O'Neal, M.R., Nearing, M.A., Vining, R.C., Southworth, J. & Pfeifer, R.A. (2005). Climate change impacts on soil erosion in Midwest United States with changes in

crop management. *CATENA*, 61 (2), 165–184. https://doi.org/10.1016/j.catena.2005.03.003
Palmer, R. S. (1964). The influence of a thin water layer on waterdrop impact forces.
Panagos, P., Ballabio, C., Borrelli, P., Meusburger, K., Klik, A., Rousseva, S., Tadić, M.P., Michaelides, S., Hrabalíková, M., Olsen, P., Aalto, J., Lakatos, M., Rymszewicz, A., Dumitrescu, A., Beguería, S. & Alewell, C. (2015). Rainfall erosivity in Europe. *Science of The Total Environment*, 511, 801–814. https://doi.org/10.1016/j.scitotenv.2015.01.008
Panagos, P., Ballabio, C., Poesen, J., Lugato, E., Scarpa, S., Montanarella, L., & Borrelli, P. (2020). A Soil Erosion Indicator for Supporting Agricultural, *Environmental and Climate Policies in the European Union. Remote Sensing*, 12(9), 1365. https://doi.org/10.3390/rs12091365
Pena, S. B., Abreu, M. M., Magalhães, M. R., & Cortez, N. (2020). Water erosion aspects of land degradation neutrality to landscape planning tools at national scale. *Geoderma*, 363, 114093. https://doi.org/10.1016/j.geoderma.2019.114093
Pianosi, F. (2014). Computational Models for Environmental Systems. In: Amigoni, F., Schiaffonati, V. (eds) Methods and Experimental Techniques in Computer Engineering. *SpringerBriefs in Applied Sciences and Technology()*. Springer, Cham. https://doi.org/10.1007/978-3-319-00272-9_1
Pilesjö, P. & Hasan, A. (2014). A Triangular Form-based Multiple Flow Algorithm to Estimate Overland Flow Distribution and Accumulation on a Digital Elevation Model. *Transactions in GIS*, 18 (1), 108–124. https://doi.org/10.1111/tgis.12015
Poesen, J. (1981). Rainwash experiments on the erodibility of loose sediments. *Earth Surface Processes and Landforms*, 6 (3–4), 285–307. https://doi.org/10.1002/esp.3290060309
Poesen, J. & Wicherek, S. (1993). Gully typology and gully control measures in the European Loess Belt. *Proceedings of International Symposium on Farm Land Erosion in Temperate Plains Environments and Hills , Date: 1992/05/01 - 1992/05/01, Location: Saint-Cloud, Paris, France*, January 1 1993. 221–239. Elsevier Science Publishers. https://lirias.kuleuven.be/1093013 [2023-07-13]
Qian, Y., Zhou, W., Yu, W. & Pickett, S.T.A. (2015). Quantifying spatiotemporal pattern of urban greenspace: new insights from high resolution data. *Landscape Ecology*, 30 (7), 1165–1173. https://doi.org/10.1007/s10980-015-0195-3
Quansah, C. (1982). Laboratory experimentation for the statistical derivation of equations for soil erosion modelling and soil conservation design. https://dspace.lib.cranfield.ac.uk/handle/1826/10343 [2023-07-30]
Rahmati, M., Neyshabouri, M.R., Fakherifard, A., Oskouei, M., Ahmadi, A. & Sheikh, J.V. (2013). Rainfall-runoff prediction using LISEM model in Lighvan watershed, North West of Iran.
Rauws, G. (1987). The initiation of rills on plane beds of non-cohesive sediments. *Catena Supplement*, (No. 8), 107–118
Renard, K. G., Laflen, J. M., Foster, G. R., & McCool, D. K. (2017). The revised universal soil loss equation. In *Soil erosion research methods* (pp. 105-126). Routledge.

Rickson, R. J. (2014). Can control of soil erosion mitigate water pollution by sediments? *Science of The Total Environment*, 468–469, 1187–1197. https://doi.org/10.1016/j.scitotenv.2013.05.057

Robinson, D.A., Panagos, P., Borrelli, P., Jones, A., Montanarella, L., Tye, A. & Obst, C.G. (2017). Soil natural capital in europe; a framework for state and change assessment. *Scientific Reports*, 7 (1), 6706. https://doi.org/10.1038/s41598-017-06819-3

Savat, J. (1982). Common and uncommon selectivity in the process of fluid transportation: field observations and laboratory experiments on bare surface.

Savat, J. & De Ploey (1982). Sheetwash and rill development by surface flow.

Savat, J., Vogt, H. & Vogt, T. (1979). Laboratory experiments on erosion and deposition of loess by laminar sheet flow and turbulent rill flow in Comptes rendus = Proceedings. *Proceedings of Laboratory experiments on erosion and deposition of loess by laminar sheet flow and turbulent rill flow in Comptes rendus = Proceedings*, 1979. 139–143. http://pascal-francis.inist.fr/vibad/index.php?action=getRecordDetail&idt=12717644 [2023-07-13]

Seeger, D.M. (2024). Understanding and preventing soil erosion.

Seibert, J. & McGlynn, B.L. (2007). A new triangular multiple flow direction algorithm for computing upslope areas from gridded digital elevation models. *Water Resources Research*, 43 (4). https://doi.org/10.1029/2006WR005128

Sparks, D.L. (2020). A golden period for environmental soil chemistry. *Geochemical Transactions*, 21 (1), 5, s12932-020-00068–6. https://doi.org/10.1186/s12932-020-00068-6

Starkloff, T. & Stolte, J. (2014). Applied comparison of the erosion risk models EROSION 3D and LISEM for a small catchment in Norway. *CATENA*, 118, 154–167. https://doi.org/10.1016/j.catena.2014.02.004

Sundborg, Å. (1956). The River Klarälven a Study of Fluvial Processes. *Geografiska Annaler*, 38 (2–3), 125–316. https://doi.org/10.1080/20014422.1956.11880887

Torri, D. & Sfalanga, M. (1986). Some Aspects of Soil Erosion Modelling. In: Giorgini, A. & Zingales, F. (eds) *Developments in Environmental Modelling*. Elsevier. 161–171. https://doi.org/10.1016/B978-0-444-99505-6.50012-5

Van Der Sande, C.J., De Jong, S.M. & De Roo, A.P.J. (2003). A segmentation and classification approach of IKONOS-2 imagery for land cover mapping to assist flood risk and flood damage assessment. *International Journal of Applied Earth Observation and Geoinformation*, 4 (3), 217–229. https://doi.org/10.1016/S0303-2434(03)00003-5

Wainwright, J. & Mulligan, M. (eds) (2012). *Environmental modelling: finding simplicity in complexity*. 2nd ed. Wiley.

Wang, S., Xu, X. & Huang, L. (2023). Spatial and Temporal Variability of Soil Erosion in Northeast China from 2000 to 2020. *Remote Sensing*, 15 (1), 225. https://doi.org/10.3390/rs15010225

Wilson, J.P., Aggett, G., Yongxin, D. & Lam, C.S. (2008). Water in the Landscape: A Review of Contemporary Flow Routing Algorithms. In: Zhou, Q., Lees, B., &

Tang, G. (eds) *Advances in Digital Terrain Analysis*. Springer Berlin Heidelberg. 213–236. https://doi.org/10.1007/978-3-540-77800-4_12
Wischmeier, W.H. & Smith, D.D. (1978). *Predicting Rainfall Erosion Losses: A Guide to Conservation Planning*. Department of Agriculture, Science and Education Administration.
Zhang, X.C. (2019). Determining and Modeling Dominant Processes of Interrill Soil Erosion. Water Resources Research, 55 (1), 4–20. https://doi.org/10.1029/2018WR023217
Zhou, Q. & Liu, X. (2002). Error assessment of grid-based flow routing algorithms used in hydrological models. International Journal of Geographical Information Science, 16 (8), 819–842. https://doi.org/10.1080/13658810210149425
Zuazo, V.H.D., Pleguezuelo, C.R.R. (2009). *Soil-Erosion and Runoff Prevention by Plant Covers: A Review*. In: Lichtfouse, E., Navarrete, M., Debaeke, P., Véronique, S., Alberola, C. (eds) *Sustainable Agriculture*. Springer, Dordrecht. https://doi.org/10.1007/978-90-481-2666-8_48

Reports and documents

FAO and ITPS (2015). *Status of the World's Soil Resources (SWSR) – Main Report*. Food and Agriculture Organization of the United Nations and Intergovernmental Technical Panel on Soils, Rome, Italy
IPBES (2018). *The IPBES assessment report on land degradation and restoration.* Zenodo. https://doi.org/10.5281/zenodo.3237393
Jetten (2018). Multi-Hazard Land Surface Process Model. Documentation & User Manual. 2nd draft. University of Twente.

Websites

European Commission (2021). *The common agricultural policy: 2023-27*. https://agriculture.ec.europa.eu/common-agricultural-policy/cap-overview/cap-2023-27_en [2024-06-03]
FAO (2020). *Global Symposium on Soil Erosion. Food and Agricultural Organization of the United Nations (FAO)*. https://www.fao.org/about/meetings/soil-erosion-symposium/key-messages/en/ [2024-03-30]
University of Twente (n.d. -b). *Flow detachment and sediment transport* https://blog.utwente.nl/lisem/basic-theory/flow-detachment-and-sediment-transport/ [2024-03-31]
University of Twente, -b (n.d.). Running LISEM. https://blog.utwente.nl/lisem/running-lisem/maps/ [2024-04-14]
SLU (n.d.). *Växtnäring och växtskyddsmedel i vatten från jordbruksmark*. https://jordbruksvatten.slu.se/vaxtnaring_start.cfm [2024-04-13]

Stockholms stad (2023). *Maximal dygnsnederbörd* https://miljobarometern.stockholm.se/klimat/klimat-och-vaderstatistik/maximal-dygnsnederbord/observatorielunden/ [2023-07-26]

Images

Pilesjö, P. & Hasan, A. (2014). A Triangular Form-based Multiple Flow Algorithm to Estimate Overland Flow Distribution and Accumulation on a Digital Elevation Model. *Transactions in GIS*, 18 (1), 108–124. [Figure 2] https://doi.org/10.1111/tgis.12015

Nilsson, H., Pilesjö, P., Hasan, A. & Persson, A. (2022). Dynamic spatio-temporal flow modeling with raster DEMs. *Transactions in GIS*, 26 (3), 1572–1588. [Figure 1,2, 3 & 5] https://doi.org/10.1111/tgis.12870

Software

ESRI (2011). ArcGIS Desktop: Release 10. Redlands, CA: Environmental Systems Research Institute.

Google (2024). Google Colaboratory. https://colab.research.google.com/

Harris, C.R., Millman, K.J., van der Walt, S.J. et al. Array programming with NumPy. Nature 585, 357–362 (2020). DOI: 10.1038/s41586-020-2649- . (https://www.nature.com/articles/s41586-020-2649-2).

JetBrains (2023). PyCharm Community Edition 2023.3

Microsoft Corporation (2018). Microsoft Excel, Available at: https://office.microsoft.com/excel

McKinney, W. & others (2010). Data structures for statistical computing in python. In Proceedings of the 9th Python in Science Conference. pp. 51–56.

Python Software Foundation. Python Language Reference, version 3.9. Available at http://www.python.org

Data sources

Digital Elevation Model (DEM). Scalgo Live. https://scalgo.com/live/. Original data source: Land survey (2019).

Property map Land data (2019). SLU Get. https://herkules.slu.se/get/. Original data source: Land Survey

Quarternary deposites 1:25 000 - 1:100 000 (2024). SLU Get. https://herkules.slu.se/get/. Original data source: Geological Survey of Sweden (SGU)

Shapefile Watershed M36. Swedish Environmental Protection Agency (2023). Provided by Stefan Andersson.

Popular science summary

Soil erosion and deposition are naturally occurring planetary phenomena. Soil can be detached from the ground (eroded) and transported in water as suspended soil particles until there is not enough energy in the water to transport the particles further. This causes particles to sink to the ground (deposit) in a new location. Soil can be detached for example by the energy of falling raindrops upon their impact on the ground, or by the energy in overland flowing water during a rain event. Soil erosion can sometimes be harmful, for example as it can cause natural disasters such as landslides or remove good soils for cultivating food on agricultural lands. Also, with climate change, predictions are that rain events will become more intense and potentially cause greater erosion than today.

Therefore, understanding which soils may be vulnerable to erosion, and where soil particles might deposit during a single rain event can give a lot of information about potential prevention measures that can be carried out. While there are models that can predict soil erosion and deposition for single rain events today, few or no such models use a dynamic triangular flow algorithm to determine how eroded soil is transported and deposited across a landscape during a rain event.

The result of this study is a prototype of a hybrid model that combines the prediction of soil erosion and deposition at a local level, depending on characteristics of the land (such as land use and soil types), and attributes of the rain event itself (such as the intensity of the rain). The prototype can account for the re-suspension and re-deposition of already deposited soil mass. It leaves room for future improvements, such as adjusting the model so that it considers how deposited soil mass changes the local heights in the landscape, which could impact how the flow of water and subsequent erosion and deposition would occur.

Acknowledgements

A great many thanks to Abdulghani Hasan, my supervisor and one of the developers of TFM-DYN, for patient and thorough guidance on a topic that was quite new to me, as well as giving me the opportunity to work on the source code of the TFM-DYN model. This project would not have been possible without your collaboration and help. Additionally, I would like to thank my professor Neil Sang for awakening my interest in GIS. Furthermore, I would like to thank my brother Daniel Haglund for assisting in the process of writing and Toon Lembrandt for assisting in the process of coding. I also want to thank Minyuan Zhang and Shivaprakash Yaragal for wonderful support.

Finally, I would also like show gratitude to the developers of LISEM, and more generally to developers of soil erosion models across the world, and for sharing information about them for others to use. This project was heavily reliant on existing works.

Publishing and archiving

Approved students' theses at SLU are published electronically. As a student, you have the copyright to your own work and need to approve the electronic publishing. If you check the box for **YES**, the full text (pdf file) and metadata will be visible and searchable online. If you check the box for **NO**, only the metadata and the abstract will be visible and searchable online. Nevertheless, when the document is uploaded it will still be archived as a digital file. If you are more than one author, the checked box will be applied to all authors. You will find a link to SLU's publishing agreement here:

- https://libanswers.slu.se/en/faq/228318.

☒ YES, I/we hereby give permission to publish the present study in accordance with the SLU agreement regarding the transfer of the right to publish a work.

☐ NO, I/we do not give permission to publish the present work. The work will still be archived and its metadata and abstract will be visible and searchable.